

MCR-84-502  
Contract No. NAS8-34679

Phase 3  
Final  
Report

January 1984

# Development of an Autonomous Video Rendezvous and Docking System

(NASA-CR-170969) DEVELOPMENT OF AN  
AUTONOMOUS VIDEO RENDEZVOUS AND DOCKING  
SYSTEM, PHASE 3 Final report (Martin  
Malletta Corp.) 105 p HC ACC/MR A01

N84-17249

Unclass

CSCI 22B G3/18 18288



**MARTIN MARIETTA**

MCR-84-502

Phase 3

Final

Contract No. NAS8-34679

Report

January 1984

---

**DEVELOPMENT OF AN  
AUTONOMOUS VIDEO  
RENDEZVOUS AND  
DOCKING SYSTEM**

John C. Tietz

**MARTIN MARIETTA AEROSPACE  
DENVER AEROSPACE  
P.O. Box 179  
Denver, Colorado 80201**

(+)

FOREWORD

---

This report presents the results of a six-month study by Martin Marietta for the National Aeronautics and Space Administration's George C. Marshall Space flight Center. The study was the third phase of Contract NAS8-34679, Development of an Autonomous Video Rendezvous and Docking System. It resulted in improvements to the spacecraft video guidance system developed under previous phases of the contract.

CONTENTS

---

	<u>Page</u>
I. SUMMARY . . . . .	1-1
II. INTRODUCTION . . . . .	II-1
III. CONCLUSIONS AND RECOMMENDATIONS . . . . .	III-1
A. New System Works with Higher Target Attitude Rates . . . . .	III-1
B. Higher Rates Require More Lights or Auxiliary RF System . . . . .	III-1
C. Field-of-View Limitations Proved Troublesome . . . . .	III-2
D. Higher Resolution Was Required . . . . .	III-3
E. Side Thrusters Were Too Weak . . . . .	III-3
F. Pounce Strategy Would Require Multiple Docking Aids . . . . .	III-4
G. Artificial Intelligence Could Help . . . . .	III-5
IV. SIMULATION RESULTS AND DISCUSSION . . . . .	IV-1
V. KALMAN FILTER IMPROVEMENTS . . . . .	V-1
A. Two Separate Filters Were Used . . . . .	V-1
B. New Filter Estimates Target Attitude and Angular Momentum . . . . .	V-2
C. Position Filter Changed Little . . . . .	V-12
D. Newton-Ralphson Iteration Improves Image Interpretation . . . . .	V-15
VI. GOAL-SELECTION STRATEGY CHANGES . . . . .	VI-1
A. Attitude Goal Selection . . . . .	VI-1
B. Translational Position Goal Selection . . . . .	VI-3
APPENDIX A	
PROGRAM LISTING . . . . .	A-1

Figure

---

II-1	Chase Vehicle Modeled in Simulation . . . . .	II-2
II-2	Three Light Docking Aid . . . . .	II-2
II-3	Scale Models and Simulator Used for Physical Simulation . . . . .	II-3
II-4	Video Processing Electronics Used in Physical Simulation . . . . .	II-4
II-5	Poor Recovery Characteristics of Old System When Docking Aid Could Not Be Seen . . . . .	II-5
II-6	Overshoot Problem with Old System . . . . .	II-6
IV-1	Typical Trajectory with Target Roll about Docking Axis . . . . .	IV-2
IV-2	Performance with Pitch and Yaw Rates of 1000 deg/h . . . . .	IV-3
IV-3	Performance with Pitch and Yaw Rates of 2000 deg/h . . . . .	IV-4
IV-4	Performance with Pitch and Yaw Rates of 3000 deg/h . . . . .	IV-5
IV-5	Performance with Pitch and Yaw Rates of 4000 deg/h . . . . .	IV-6
IV-6	Recovery from Docking Aids Rolling Out of Sight . . . . .	IV-7

Table

---

IV-1	Measurement Errors . . . . .	IV-1
IV-2	Comparison of Fuel Use and Time of Flight for Old and New Systems . . . . .	IV-7



# Summary



I. SUMMARY

---

Improvements have been made to the video rendezvous and docking system developed under this contract. The changes allow the system to dock with targets tumbling twice as fast as the old system could accommodate. They also improve reliability at lower tumble rates. The improved performance results from:

- 1) Adding a second Kalman filter to improve estimates of target attitude and allow anticipation of target attitude changes;
- 2) Changing the guidance strategy to make use of the data from the Kalman filter.

Other minor changes were made to improve performance. Larger thrusters were used on the sides of the chase spacecraft, and a higher-resolution (broadcast quality) television camera replaced the original 128-line camera.

Improving performance further will probably require multiple docking aids or an auxiliary radio frequency (RF) system, because the system is now limited primarily by the docking aid rolling out of sight behind the target. Although the Kalman filter allows dead reckoning, the accuracy of its position estimates deteriorates with time, especially when the chase spacecraft attempts to maneuver around the target.

Application of artificial intelligence in the guidance system might minimize this problem, and precision accelerometers could slow the growth of estimation error. However, the problem will still be difficult to solve without some form of additional sensor data from the back side of the target spacecraft.

# Introduction



## II. INTRODUCTION

---

The study reported here was the third phase of a contract to investigate techniques that could be used in an autonomous video rendezvous and docking system for spacecraft.

Under the first phase of the contract, we identified several techniques that appeared suitable for such a system, defined the equations and algorithms these techniques would use, and evaluated video guidance control systems based on these techniques through computer simulation.

To ensure that practical problems were considered, the simulation modeled not only the sensor, but also methods for dealing with a number of practical problems, e.g., maintaining control when the target spacecraft leaves the field of view of the guidance sensor. The simulation also modeled the characteristics and limitations of practical spacecraft to reveal subtle incompatibilities that might otherwise go unnoticed. A mission model was defined to serve as a basis for the simulation.

In this model, the chase vehicle (Fig. II-1) is a general-purpose spacecraft for repair, refurbishment, and retrieval of other spacecraft. After it is deployed from the Space Shuttle, it must rendezvous and dock with the long-duration exposure facility (LDEF), which, it is assumed, has been modified for this operation and is in a circular orbit at an altitude of 300 km. We will refer to LDEF as the target spacecraft, because, although a specific mission model was used for the simulations, the intent was that the guidance method be usable on a variety of spacecraft.

In the second phase of the contract, we conducted a physical simulation of the best technique evaluated under the first phase. This technique used a docking aid comprising three flashing lights mounted on the target spacecraft (Fig. II-2). The appearance of this pattern of lights uniquely defines both the relative positions and the relative attitudes of the two spacecraft.

UNCLASSIFIED  
OF PGOR Q...

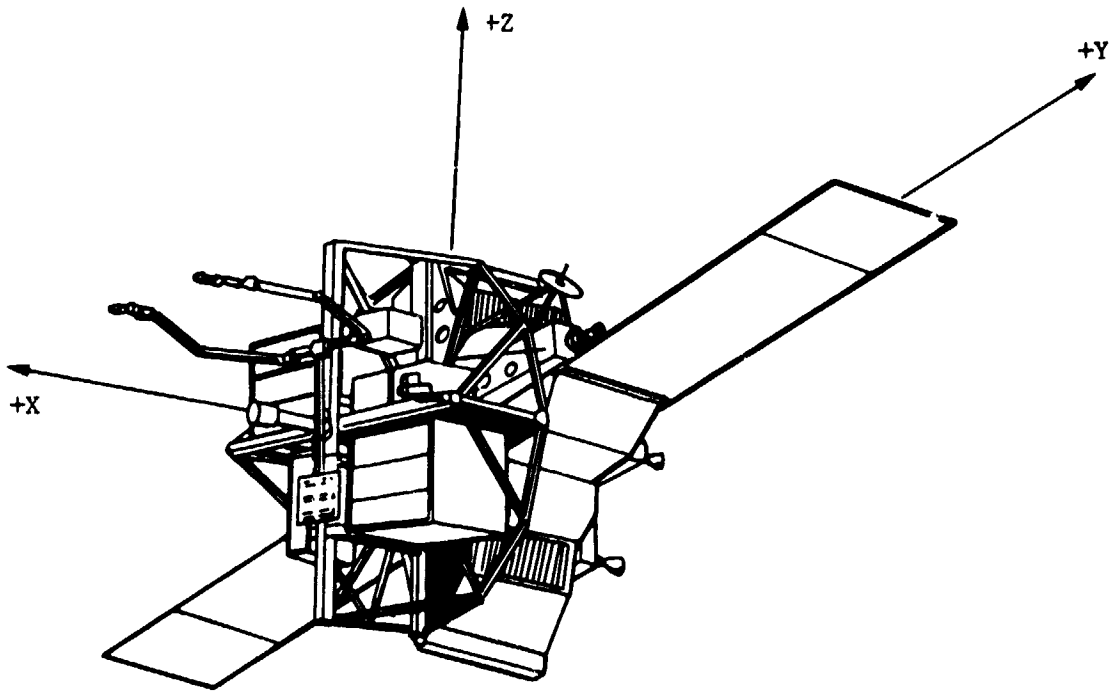


Figure II-1 Chase Vehicle Modeled in Simulation

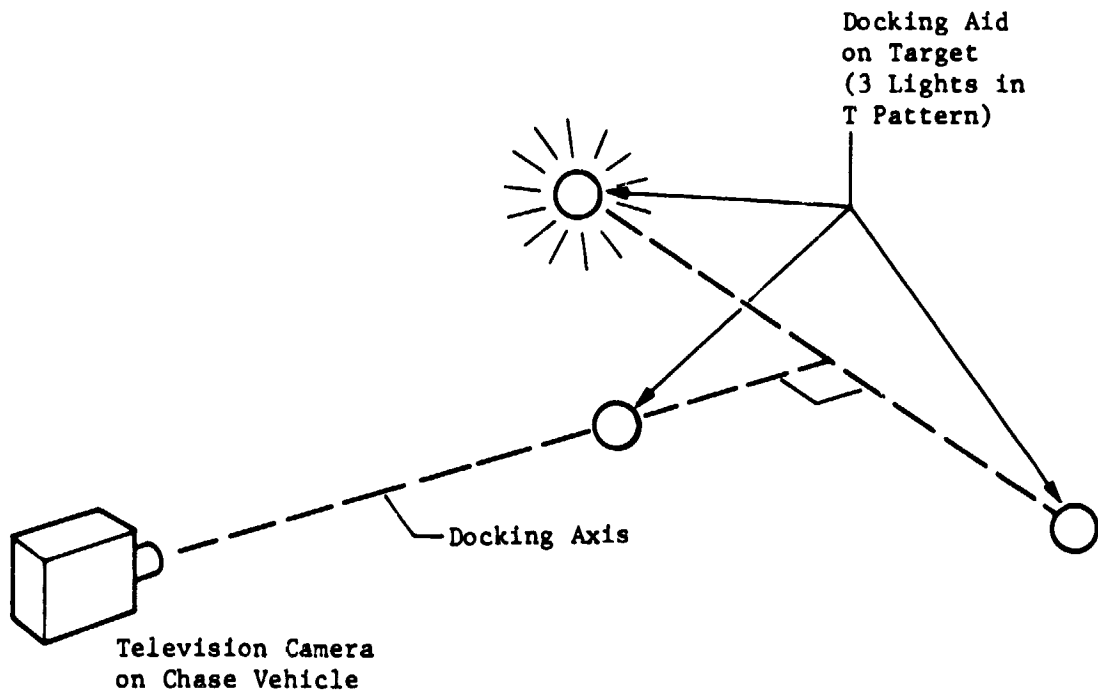
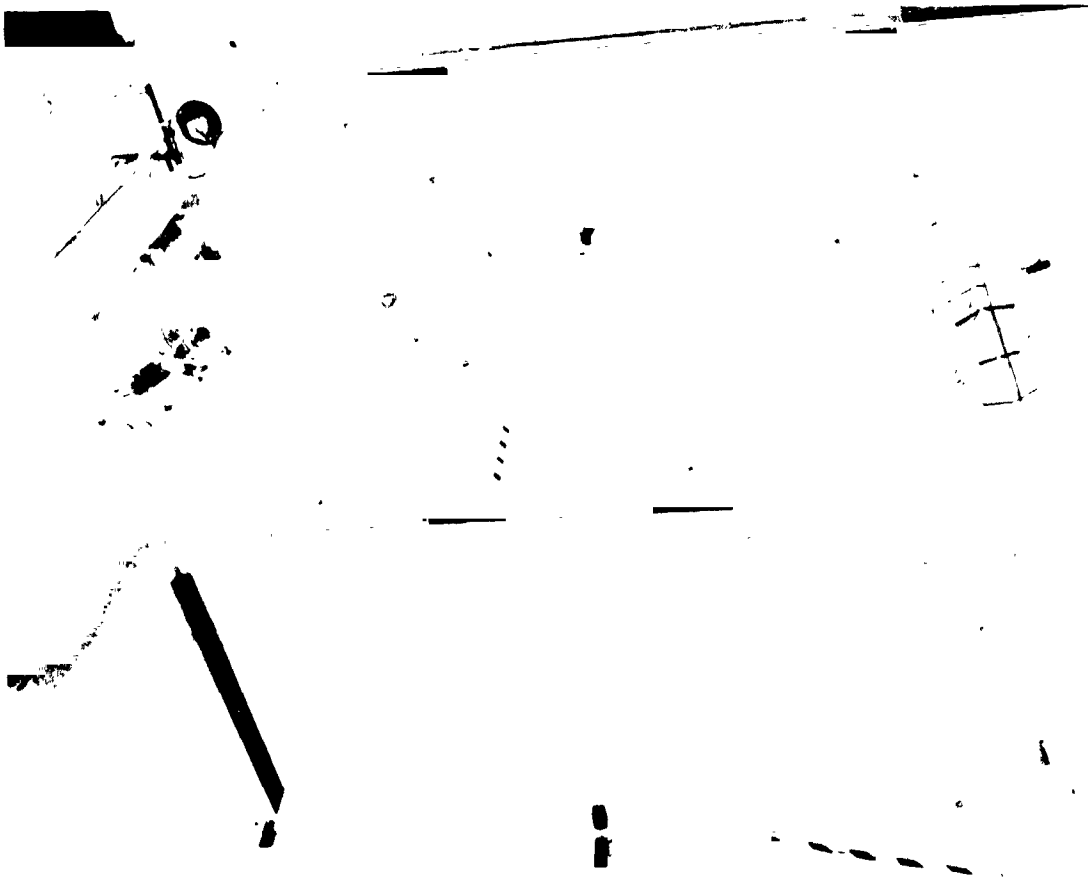


Figure II-2 Three Light Docking Aid

ORIGINAL PAGE IS  
OF POOR QUALITY

To simulate the entire operation from a range of 300 m to contact, three target-spacecraft models were required (Fig. II-3). Each model was built to a different scale and was used in a different part of the simulation. The smallest model was 1/100 scale and was used for ranges greater than approximately 30 m. A 1/10 scale model was used to simulate ranges between 3 and 30 m. For the final seconds of the docking operation, a full-scale model of a portion of one side of LDEF was used.



*Figure II-3 Scale Models and Simulator Used for Physical Simulation*

To simulate the servicer spacecraft (chase vehicle), we mounted a television camera on a six-degree-of-freedom simulator. The simulation computer sent servo commands to position the camera so that the television image would correspond to what a flight camera on a real chase vehicle would see. Video processing electronics (Fig. II-4) converted

the imagery to a set of statistics that a computer can quickly analyze to determine the relative positions and attitudes of the two spacecraft. These statistics were transmitted to the simulation computer, which modeled the activity of the simulated flight computer and the dynamics of the two spacecraft.

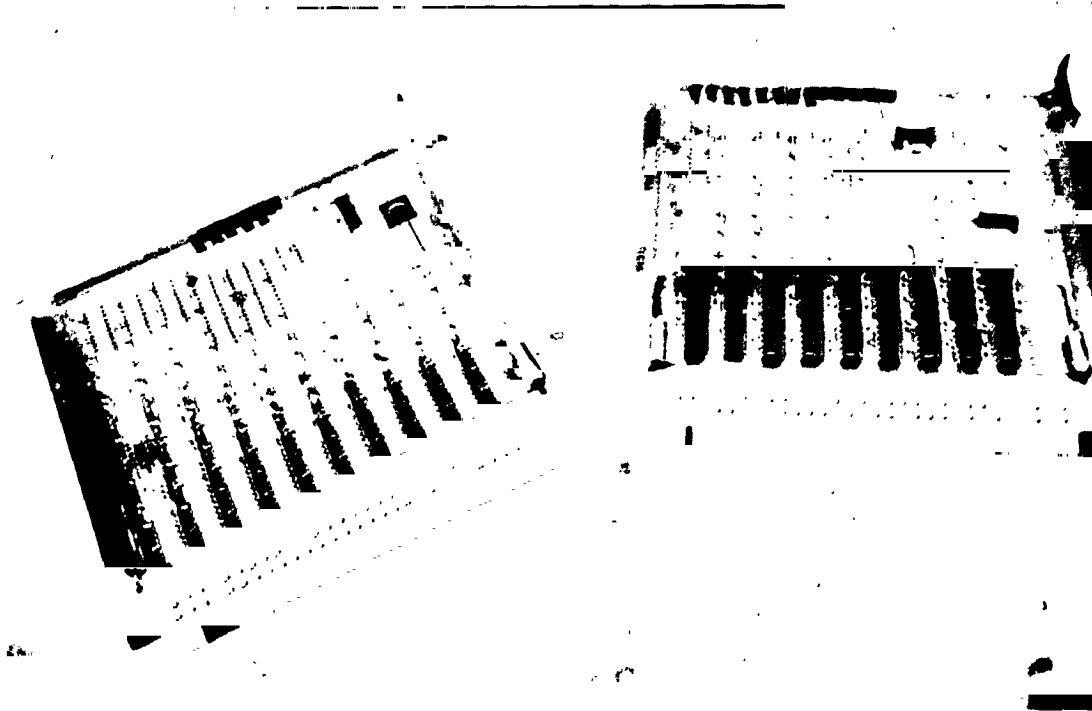


*Figure II-4 Video Processing Electronics Used in Physical Simulation*

Although the work under these two phases demonstrated the apparent practicality of a video guidance system, improvements were required for docking with tumbling spacecraft. The original system was unable to cope with target attitude rates materially over 1000 deg/h, and was unreliable at this rate.

Part of the problem was that the Kalman filter, which the guidance system used for dead reckoning, did not keep track of target attitude. This made it nearly impossible for the chase vehicle to recover gracefully when the docking aid on the target rotated out of view behind the target (Fig. II-5).

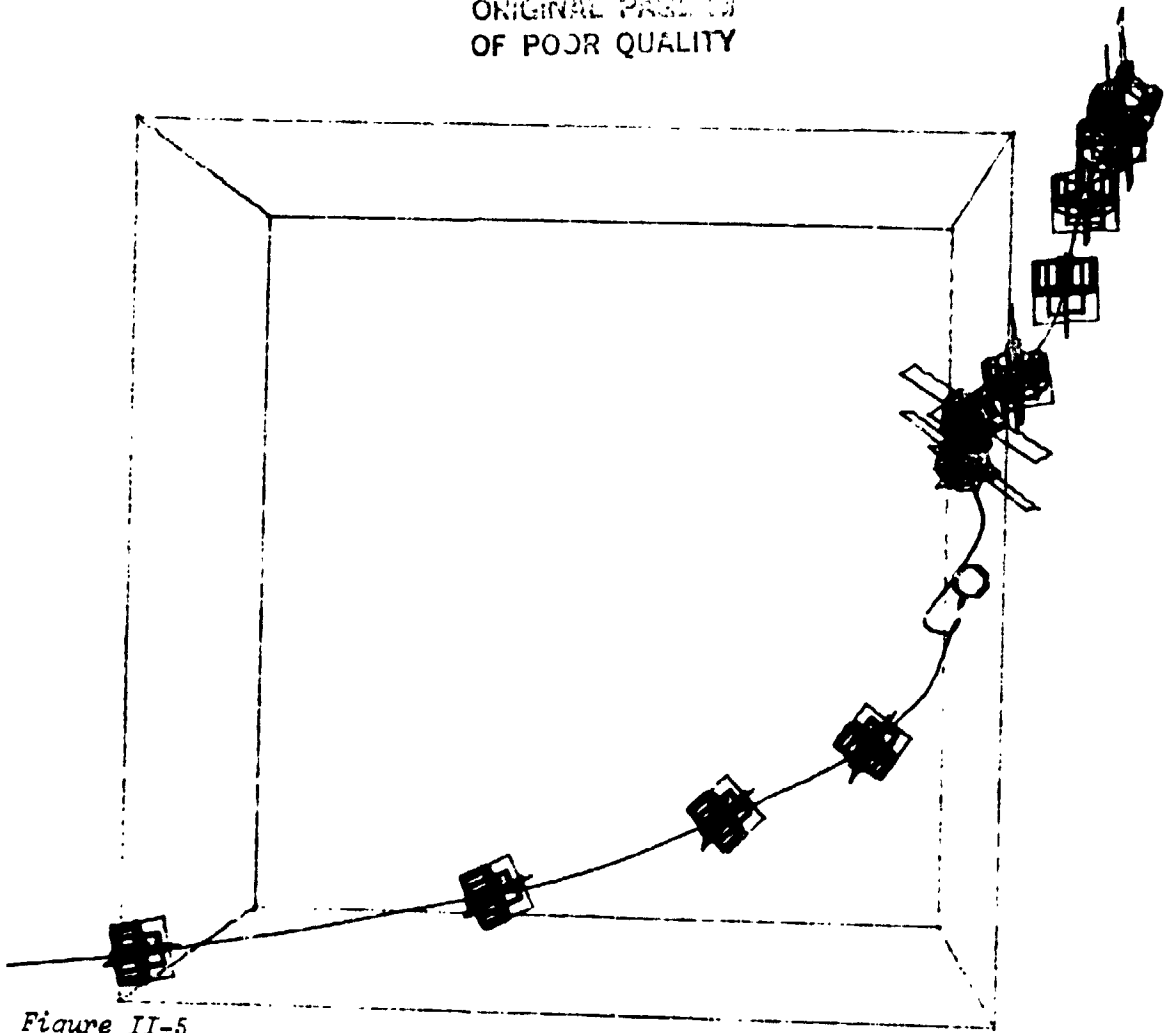


*Figure II-5  
Poor Recovery Characteristics of Old System When Docking Aid Could Not  
Been Seen*

Another problem was strategy logic that did not plan ahead for a rotating target: the chase vehicle built up too much speed in approaching the target, using powerful thrusters at the rear of the spacecraft. When it arrived in the vicinity of the target, the target had rotated, and the chase vehicle had to fly sideways for the last few meters. It was then unable to stop quickly enough with the weaker side thrusters and overshot the target (Fig. II-6).

The activity under Phase 3 addressed these shortcomings by making improvements in the strategy logic and augmenting the Kalman filter to estimate target attitude and tumble rate.

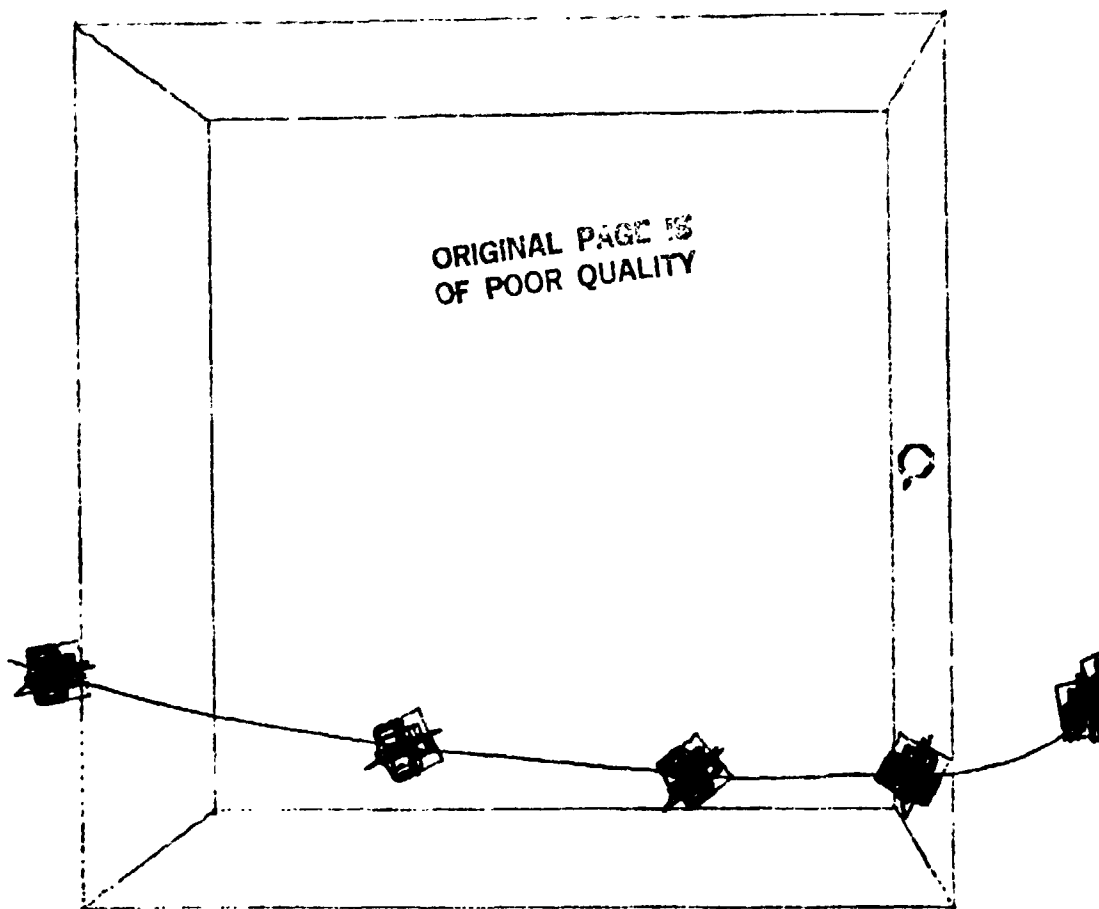


*Figure II-6 Overshoot Problem with Old System*

This report concentrates on the third phase of the contract and does not repeat very much of the information that was published in the final reports for Phases 1 and 2. The reader who has not read those reports will find it advantageous to read them before reading the more technical sections of this volume.

# Conclusions and Recommendations

Conclusions and  
Recommendations



### III. CONCLUSIONS AND RECOMMENDATIONS

---

#### A. NEW SYSTEM WORKS WITH HIGHER TARGET ATTITUDE RATES

The changes made under this contract phase have approximately doubled the tumble rates the chase vehicle can accommodate. This improvement was achieved primarily by:

- 1) Adding a second Kalman filter, which estimates target attitude and angular momentum;
- 2) Changing the goal-selection and attitude error computations.

The system now works reliably at rates up to 1000 deg/h and, depending on initial conditions, can cope with rates up to 4000 deg/h.

#### B. HIGHER RATES REQUIRE MORE LIGHTS OR AUXILIARY RF SYSTEM

The main factor that now limits rates the system can accommodate is the fact that the docking aid on the target rotates out of view before the chase vehicle can get close to the target. The result is that the chase vehicle must fly a significant distance on dead reckoning. It can do this for a short time, but maneuvering to the far side of the target requires considerable use of its thrusters.

Unfortunately, each time the thrusters are used, the system loses confidence in its position and velocity estimates. This is because the velocity change that results from thruster operation cannot be predicted or measured exactly. The thruster may produce slightly more or less thrust than was anticipated. To be safe, the guidance strategy must take this loss of confidence into account and back away from the target.



If the system cannot get another measurement for an extended period, it must retreat a considerable distance from the target. It is then in a poor position for a second approach when the docking aid is again visible.

If multiple docking aids were provided, the system could always get a position update and would not have to back away from the target. The result would be:

- 1) A significant savings in fuel consumption;
- 2) Shorter time of flight;
- 3) Greatly increased reliability;
- 4) Ability to accommodate significantly higher tumble rates.

An alternative method of avoiding the problem is an auxiliary RF guidance system that could provide at least range and direction to the target when the docking aid is out of view. Precision accelerometers in the existing system would also help by slowing the growth of estimation error.

#### C. FIELD-OF-VIEW LIMITATIONS PROVED TROUBLESOME

During the physical simulations under the second contract phase, we found that two different camera lens focal lengths were required. This requirement was confirmed under the current study. At great distances from the target, the system needs a lens with a long focal length to resolve details on the docking aid. At close range, however, such a lens becomes a problem; because of transient attitude excursions, portions of the docking aid frequently leave the camera's field of view. The system then cannot take new measurements and must back away from the target as its position estimation accuracy deteriorates.

We solved this problem by switching focal lengths at a range of 15 m. Alternately, the problem might be solved by using a second, smaller, docking aid, which would be activated after the chase vehicle approached within approximately 15 m. However, even a very small docking aid could leave the field of view of a long lens. Switching lenses appears to be the more practical solution.

D. HIGHER RESOLUTION WAS REQUIRED

We found it necessary to increase the camera resolution to approximately that of commercial broadcast cameras to cope with high tumble rates. The reason was that at rates over approximately 2000 deg/h, the docking aid often rotates out of sight behind the target before the chase vehicle gets close enough to get precision measurements with a lower resolution camera. If it is to go on dead reckoning for a significant distance, starting with a good initial state estimate is vital. The 128-line camera modeled in previous simulations did not provide a good enough estimate.

E. SIDE THRUSTERS WERE TOO WEAK

We found it necessary to increase the thrust authority of the thrusters on the top, bottom, and sides of the chase vehicle. There was a great difference in authority between these thrusters and those mounted on the front and back of the vehicle (an 8 to 1 ratio). The result was that the chase vehicle tended to greatly overshoot the target when it had to brake with the side-mounted thrusters. Part of this problem could be solved by changes to the control law, but these changes were not particularly effective.

At the same time, we increased the torque authority to cure problems with the docking aid leaving the field of view for extended periods during maneuvers.

F. POUNCE STRATEGY WOULD REQUIRE MULTIPLE DOCKING AIDS

During this study, astronauts were practicing with the Manned Maneuvering Unit simulator at Martin Marietta Denver Aerospace. They were training for a mission in which they are to dock with the Solar Maximum Spacecraft, which is, at the time of this writing, tumbling in orbit due to a malfunction. The similarity between their mission and the mission model for the video rendezvous system suggested that we should try to adopt techniques they found effective.

One of the things they learned was that it was most effective to stop at a convenient position close to the target spacecraft and wait for an opportune moment. They would then pounce on the target from close range, matching the tangential velocity component only during the last seconds of flight.

We incorporated this technique into the simulation program and ran a number of simulations. The results were disappointing.

The reason the technique failed became quite obvious: while the chase vehicle was waiting to pounce, the docking aid was on the opposite side of the target spacecraft. Because the system gets data only from observing the docking aid, it had to operate on dead reckoning for two minutes or more. As its confidence in its position deteriorated, it backed away from the target to prevent collision. In doing so, it used its thrusters, and the thrust uncertainty further reduced its confidence in its position estimate. As a result, it backed farther and farther from the target, so when the docking aid was again visible, the chase vehicle was as far from the target as when the simulation started. It went through cycles of approaching and retreating until it ran out of fuel.

The astronauts did not have this problem because they could obtain as much position data from the back side of the target as from the front.

(+)

If the chase vehicle could see several docking aids at various locations on the target, it too might be able to make effective use of the strategy. However, with a single docking aid, the most effective approach was to keep the docking aid in view as much as possible.

G. ARTIFICIAL INTELLIGENCE COULD HELP

One of the shortcomings of the guidance system is its inability to reason about the following:

- 1) Long-range goals - The guidance system treats each decision interval of approximately 1.2 s as a separate problem. It does not plan an optimal trajectory and stick to it; it does not think about the long-range consequences of its decisions. As a result, it often wastes time and fuel in undoing its previous actions.
- 2) Interaction of goals - The system knows that it must back away from the target for safety when it cannot see the docking aid. But in deciding to back away, it does not consider how much doing so will degrade its position estimates. By reasoning about this, it might decide to postpone the use of thrusters.
- 3) Alternate strategies - Although the algorithm used in the system does consider a variety of factors (safety, control loop bandwidth requirements, anticipated target motion) it is still a single strategy. The system does not predict the results of alternative strategies and select one. A system that considered alternative plans might perform better.

Although much of the reasoning process for an intelligent guidance system would require numerical computation, a large portion of the task involves symbol manipulation, tree-searching, backtracking and other operations that are difficult to perform in most computer languages. For example, a program to search a decision tree is easiest to write and understand if the computer language used allows recursive function

calls, flexible data structures, and automatic garbage collection. FORTRAN is weak in all these operations, and although C and PL/I support some of them, these languages do not offer the flexibility of LISP and its derivatives in solving problems of this type.

A reasonable next step in developing a better guidance system would be to analyze the knowledge-base requirements of such a system and develop knowledge-representation schemes for automated reasoning about the factors discussed previously.



# Simulations Results and Discussion



IV. SIMULATION RESULTS AND DISCUSSION

Although almost all the improvement in measurement accuracy in the new system (Table IV-1) can be attributed to the higher resolution television camera, the new system had much better control accuracy. The old system would often dock with more than 45-deg misalignment at target attitude rates as low as 500 deg/h, and at 1000 deg/h, it rarely docked with misalignment less than 15 deg. Furthermore, at rates of 1000 deg/h and above, it frequently crashed into the target or let the target get out of its field of view long enough that it was not able to recover.

Table IV-1 Measurement Errors

Range (m)	Position Errors (m)		Attitude Error (deg) Pitch, Yaw, or Roll ( $1\sigma$ )
	Along Chase Vehicle x-Axis ( $1\sigma$ )	Along Chase Vehicle y- and z-Axes ( $1\sigma$ )	
10	0.141	0.100	0.362
25	0.318	0.0964	0.628
50	1.76	0.303	0.941
100	9.80	0.970	1.85
286	117	6.32	9.33

The new system's performance at these rates is illustrated in the trajectory plots in Figures IV-1 through IV-5. In each of the simulations illustrated, the chase vehicle started from a randomly selected position approximately 300 m from the target. Because problems rarely developed until the range was reduced to 30 or 40 m, the figures show only the last 60 m of the flight. The boxes shown in the figures represent a 60-m cube. Its primary use was to enhance depth perception when stereo pairs of plots were viewed while we were running the experiments.

The primary reason for docking failures at the higher rates was the docking aid's rolling out of sight before the chase vehicle could get close enough to prevent it. This fact is illustrated dramatically in

ORIGINAL PAGE IS  
OF POOR QUALITY

Figure IV-3: with a target tumble rate of 2000 deg/h, the lights often rotated out of sight while the chase vehicle was still some distance away. Because the tumble rate was low, the lights did not reappear for six minutes. By this time, the chase vehicle's state estimate had badly deteriorated. Although the chase vehicle was often able to recover from this by going around the target (Fig. IV-6a) or waiting for the docking aid to reappear (Fig. IV-6b), it generally used an excessive amount of fuel (Table IV-2). The success rate at 2000 deg/h was actually lower than at 3000 deg/h.

Note:

Neither system had trouble with roll about the docking axis.  
The study therefore concentrated on pitch and yaw axes.

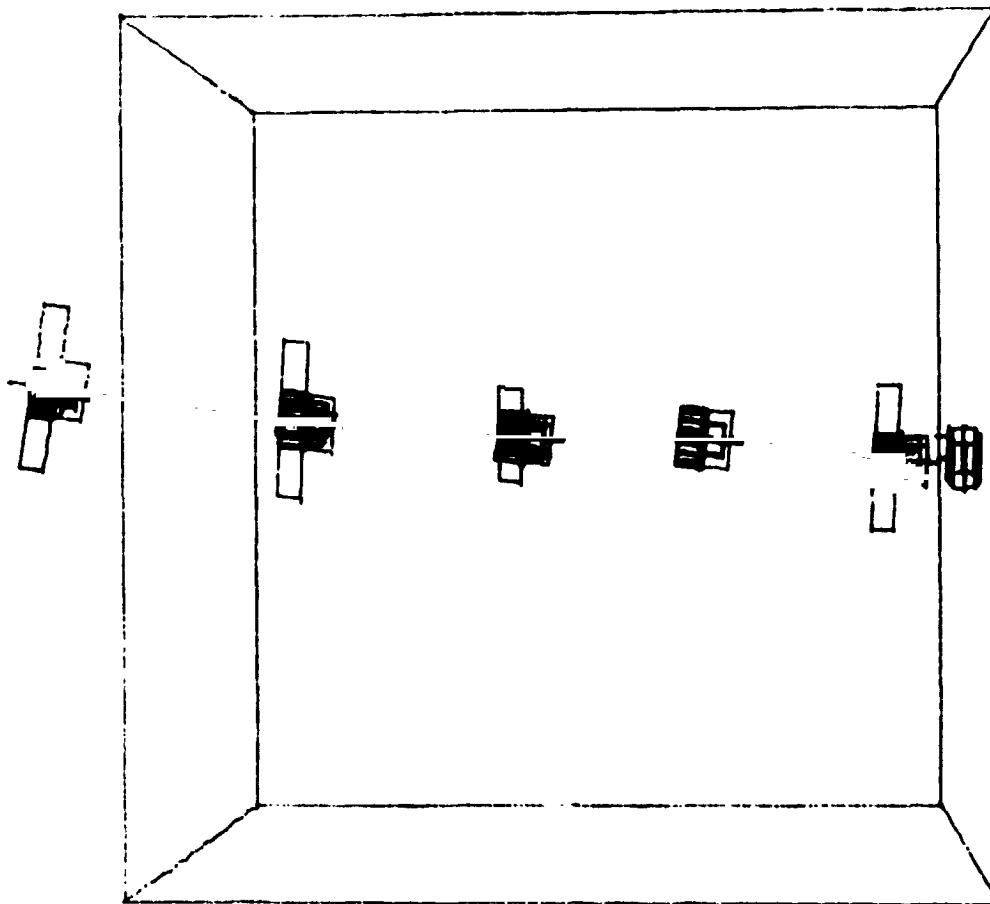


Figure IV-1 Typical Trajectory with Target Roll about Docking Axis



(+)

# OF THE OF POOR QUALITY

**Note:**  
In (a) through (d), the pitch axis was the tumble axis. In (e) and (f), the target tumbled about its yaw axis.

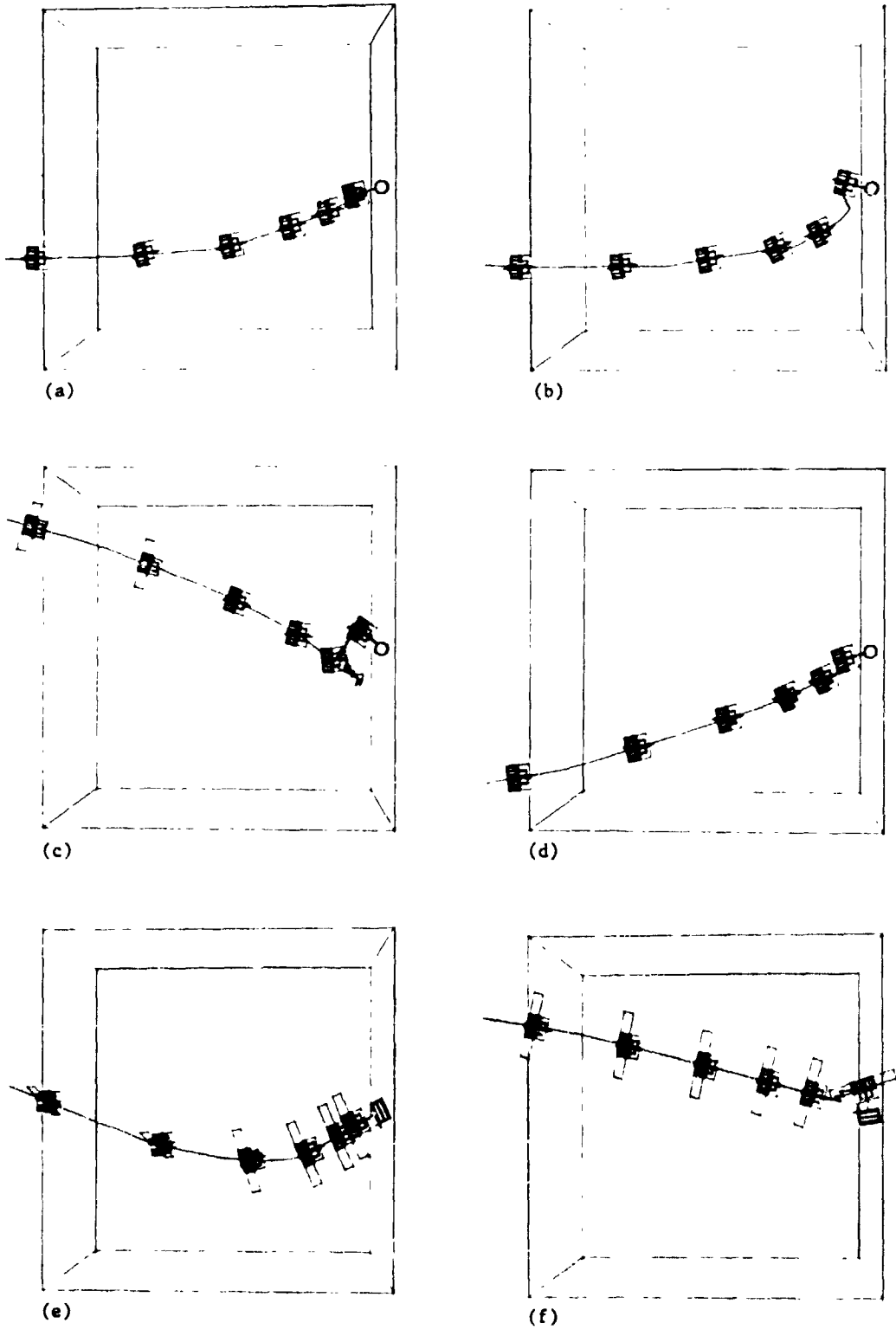


Figure IV-2 Performance with Pitch and Yaw Rates of 1000 deg/h

ORIGINAL PAGE IS  
OF POOR QUALITY

Note:

A rate of 2000 degrees per hour was the most troublesome, because the docking aid was out of sight for the longest time. In (a) and (b), the pitch axis was the tumble axis; in (c)-(f), the yaw axis was the tumble axis: Simulations (b), (e), and (f) were stopped when an arbitrary time limit was reached.

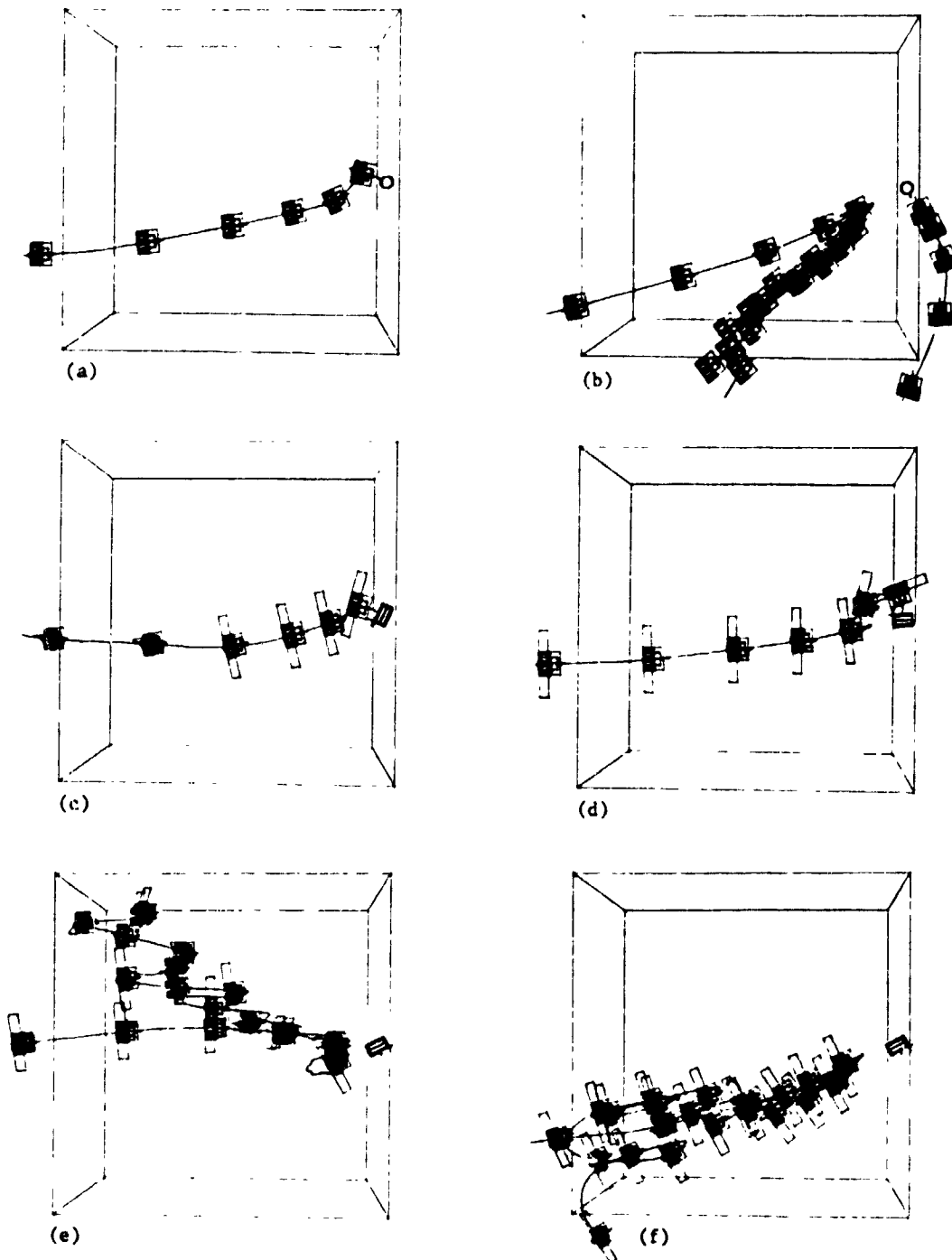


Figure IV-3 Performance with Pitch and Yaw Rates of 2000 deg/h

ORIGINAL FIGURE IS  
OF POOR QUALITY

Note:

Tumble axis was pitch axis in (a), yaw in others.

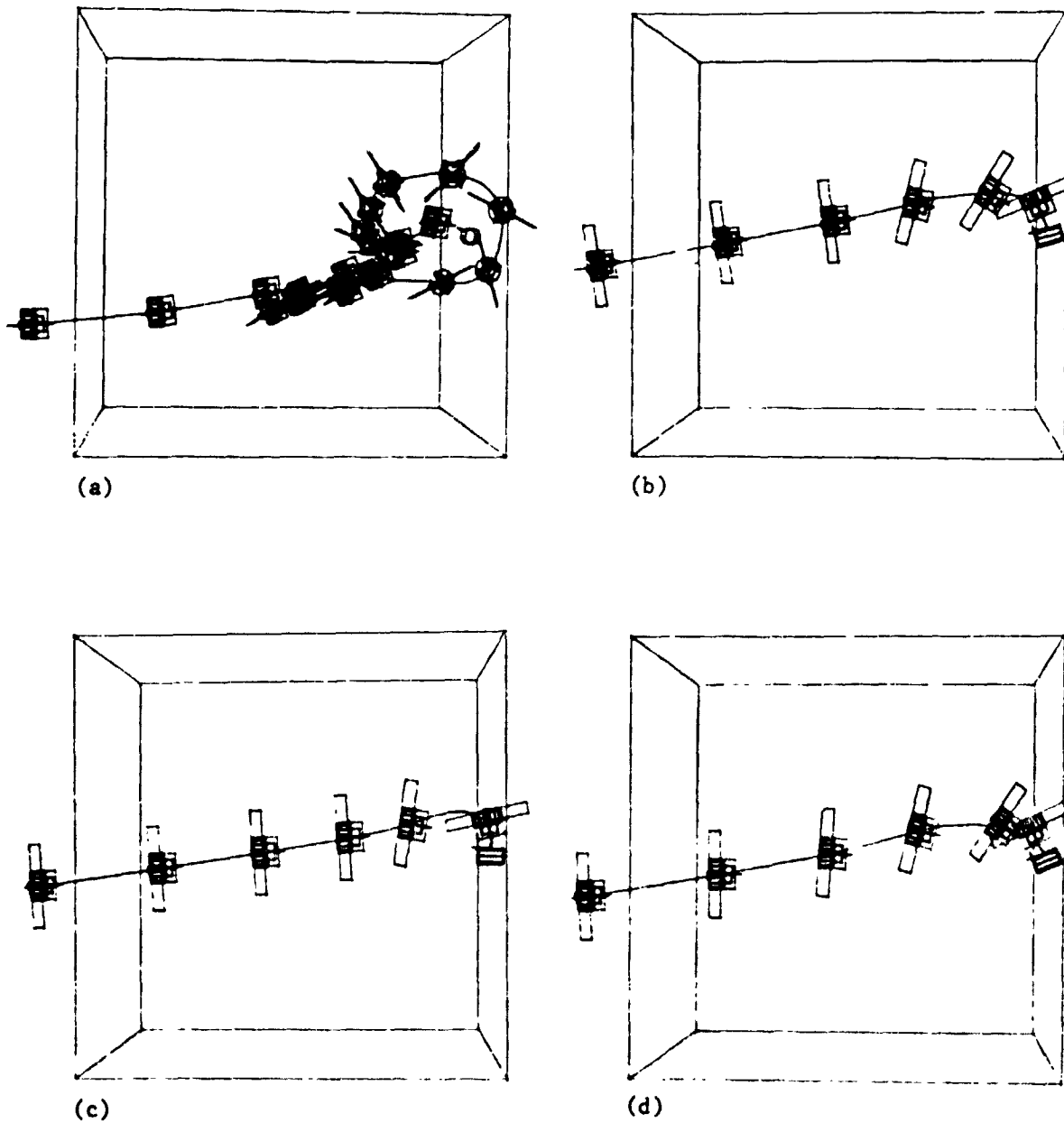


Figure IV-4 Performance with Pitch and Yaw Rates of 3000 deg/h

Note:

In (a) and (b), the tumble axis was the yaw axis; in (c)-(f) the tumble axis was the pitch axis. Simulation (e) was stopped when an arbitrary time limit was reached. In (f), the chase vehicle docked, but misalignment was extreme.

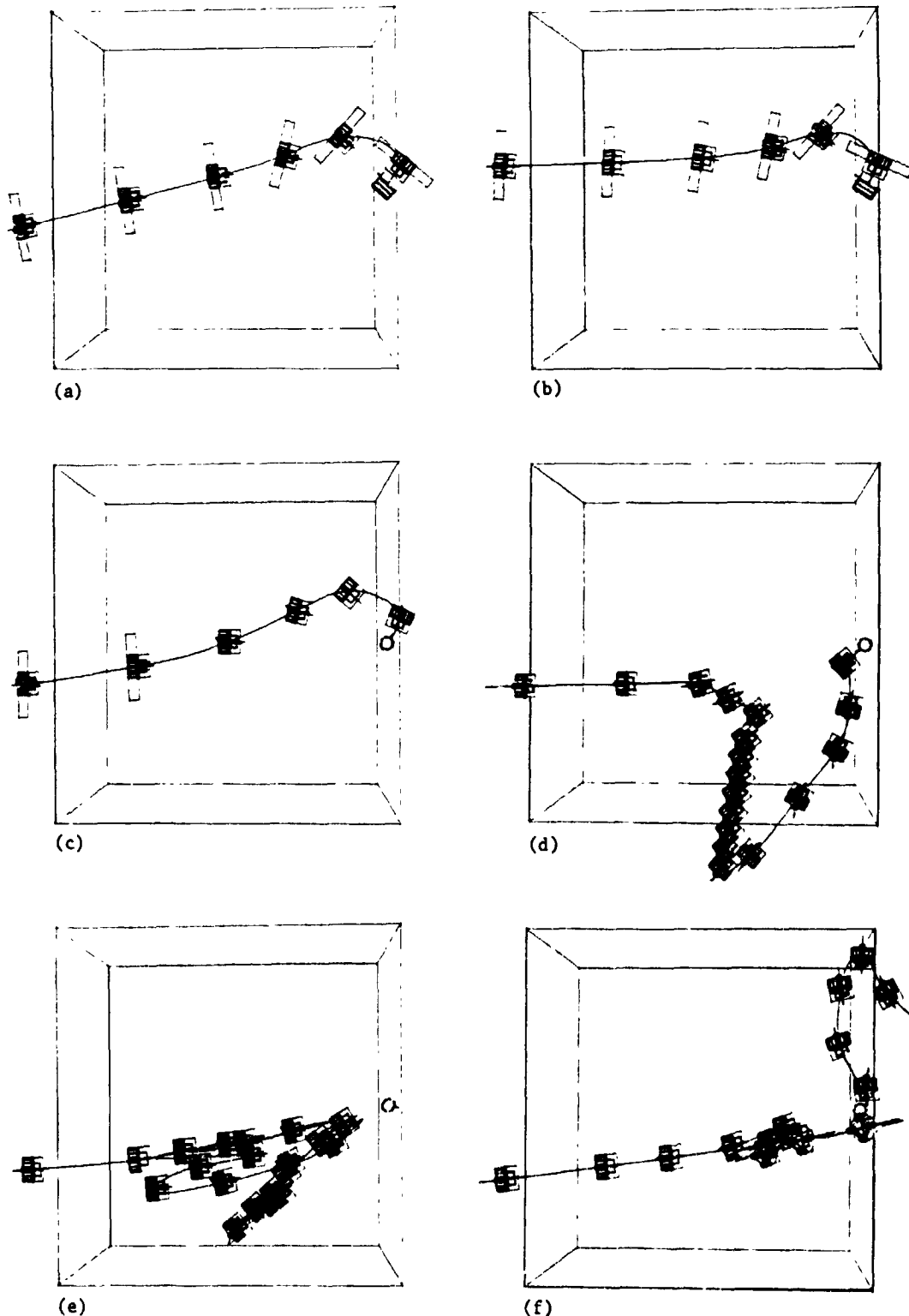


Figure IV-5 Performance with Pitch and Yaw Rates of 4000 deg/h

Note:

In (a) the chase vehicle found a path around the target. More frequently it did not but waited for the docking aid to reappear (b).

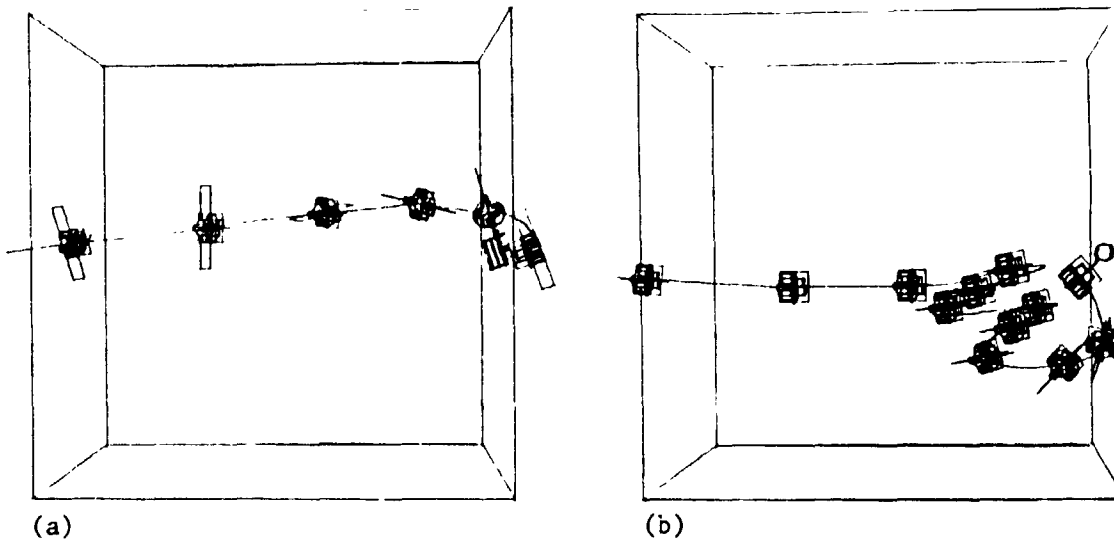


Figure IV-6 Recovery from Docking Aids Rolling Out of Sight

Table IV-2

Comparison of Fuel Use and Time of Flight for Old and New Systems

Pitch or Yaw Rate (deg/h)	Old System		New System	
	Median Time (s)	Median Fuel Consumption (Kg)	Median Time (s)	Median Fuel Consumption (Kg)
1000	192	28.4	227	53.9
2000	279	54.7	∞*	∞*
3000	201	27.2	∞*	∞*
4000	201	31.2	∞*	∞*

\*Chase vehicle did not appear to have a chance of docking after 280 seconds of flight. Simulation terminated.

We partially succeeded in overcoming this problem by using a goal-modification strategy. The guidance logic analyzed the shortest path from the current position to the docked position. If it found that the path would pass too close to the target, it attempted to select an alternative near-term goal on the shortest circular path around the target at an acceptable radius. This approach was not as successful as we had hoped. It appears that in pursuing the new goal, it had to make large velocity adjustments, which resulted in increased uncertainty in its position knowledge. It then had to back away from the target for safety.

The largest contributor to fuel savings in docking with slowly tumbling targets was the widened deadband allowed in the new control system. The improvement was not large, but it was noticeable.

# Kalman Filter Improvements

V. KALMAN FILTER IMPROVEMENTS

---

A. TWO SEPARATE FILTERS WERE USED

The original simulation program used a Kalman filter that estimated only position and velocity. The guidance algorithm was based on an assumption that the attitude measurements were accurate enough without filtering. The disadvantages of this scheme became apparent when significant target attitude rates were simulated: because the chase vehicle could not anticipate the motion of the docking fixture, it always headed toward the instantaneous docking-port position, not toward where the port would be at the time of arrival. When the attitude rate exceeded 1000 to 2000 deg/h about either the pitch or yaw axis, the guidance algorithm was not able to cope. The chase vehicle either circled the target indefinitely or crashed into the target. Furthermore, the chase vehicle's attitude control algorithm used the video imagery for guidance, attempting to keep the light pattern in the middle of the field of view. This strategy caused problems when the target was tumbling, because centering the lights in the field of view did not guarantee that the docking fixtures would be aligned.

The modified guidance system solves both of these problems, and the key to the solution was an expansion of the Kalman filter to include attitude and attitude rate in addition to translational quantities.

The first design decision was whether to add state elements to the existing Kalman filter or to split the problem into two independent sub-problems, chase vehicle position, and target attitude. We considered the increase in burden on the flight computer, the likelihood of filter stability problems, the degree of coupling between position and attitude measurements, and the absence of coupling between position dynamics and attitude dynamics.



We concluded that if we could reduce the measurement coupling, two filters would give essentially the same accuracy as a single larger filter, but with less likelihood of instability problems and with a significant reduction in the burden on the flight computer.

Therefore, only slight modifications were made to the original position filter, and an independent target-attitude filter was added.

## B. NEW FILTER ESTIMATES TARGET ATTITUDE AND ANGULAR MOMENTUM

For state variables, the added filter uses a quaternion and an angular momentum vector. Attitude is expressed with respect to the nonrotating primary reference frame used for chase vehicle guidance. The angular momentum vector is also expressed in this frame.

### 1. Selection of State Variables

We selected the quaternion parameterization of attitude to minimize the computational burden. The other parameterizations we considered were:

- 1) A set of three angles, e.g., yaw, pitch, and roll;
- 2) The Gibbs vector parameterization;
- 3) A direction cosine matrix;
- 4) Euler axis and angle;
- 5) The first three elements of a quaternion.

The three-angle parameterization was rejected because it requires complex formulas for use. For example, the simplest way to propagate the state estimate is to convert to one of the other parameterizations. Furthermore, the approach requires added logic to handle exceptions at singularities.

We rejected the Gibbs vector approach for the same reasons: the complexity of the formulas and the presence of a singularity that requires special handling.

Direction cosine matrices have three disadvantages. First, they have nine elements to compute, six of which are redundant. Second, the propagation formula requires approximately 30% more arithmetic than the formula for quaternions. Third, they require much more arithmetic than quaternions do for incorporating a new measurement.

The remaining two options were rejected because the simplest way to use them is by converting to quaternions for computations and then converting back to the original form. For example, the first three (or any three) elements of a quaternion can be used to express attitude in the theoretical minimum number of elements as long as the sign of the fourth element is known. This is true because the sum of the squares of the elements always equals 1.0. Because multiplying all four elements of a quaternion by -1.0 does not change the attitude expressed, it is always possible to manipulate the quaternion so that the last element is positive. When this is done, the last element is completely redundant and can be dropped. However, there is little to be gained by dropping an element and much to lose. The simplest way to use the three remaining elements is to recreate the fourth element. Furthermore, when this element is small, roundoff errors will prevent accurate reconstruction.

In summary, the quaternion representation appeared to be best for this application. Therefore, the first four state variables are the four elements of the quaternion that represents the target's attitude with respect to the primary reference frame.

The next three elements were to be some measure of attitude rate, which can also be parameterized in different ways. We considered:

- 1) The angular velocity vector in the current target reference frame;

- 2) The angular velocity vector in the primary frame;
- 3) The angular momentum vector in the current target frame;
- 4) The angular momentum vector in the primary frame.

We selected the angular momentum vector, expressed in the primary frame, because this vector does not change with time. This fact simplified state estimate propagation and anticipation of target attitude changes in the guidance strategy algorithm. In addition, this parameterization made it easier to analyze the filter's accuracy, stability, and rate of convergence while we were running simulations.

The remaining three elements of the state vector, then, are the x, y, and z components of the target's angular momentum vector, expressed in the primary reference frame. This makes a total of seven state variable elements. In the simulation program, they are the seven elements of the array ESTA.

## 2. State Estimate Propagation

Between observations, the filter propagates the state estimate covariance by linearizing about the current estimate. To do this, it computes a matrix of partial derivatives, F:

$$[1] \quad F = \begin{bmatrix} \frac{\partial \dot{x}_1}{\partial x_1} & \frac{\partial \dot{x}_1}{\partial x_2} & \frac{\partial \dot{x}_1}{\partial x_3} & \frac{\partial \dot{x}_1}{\partial x_4} & \frac{\partial \dot{x}_1}{\partial x_5} & \frac{\partial \dot{x}_1}{\partial x_6} & \frac{\partial \dot{x}_1}{\partial x_7} \\ \frac{\partial \dot{x}_2}{\partial x_1} & \frac{\partial \dot{x}_2}{\partial x_2} & \frac{\partial \dot{x}_2}{\partial x_3} & \frac{\partial \dot{x}_2}{\partial x_4} & \frac{\partial \dot{x}_2}{\partial x_5} & \frac{\partial \dot{x}_2}{\partial x_6} & \frac{\partial \dot{x}_2}{\partial x_7} \\ \frac{\partial \dot{x}_3}{\partial x_1} & \frac{\partial \dot{x}_3}{\partial x_2} & \frac{\partial \dot{x}_3}{\partial x_3} & \frac{\partial \dot{x}_3}{\partial x_4} & \frac{\partial \dot{x}_3}{\partial x_5} & \frac{\partial \dot{x}_3}{\partial x_6} & \frac{\partial \dot{x}_3}{\partial x_7} \\ & & & \cdot & & & \\ & & & \cdot & & & \\ \frac{\partial \dot{x}_7}{\partial x_1} & \frac{\partial \dot{x}_7}{\partial x_2} & \frac{\partial \dot{x}_7}{\partial x_3} & \frac{\partial \dot{x}_7}{\partial x_4} & \frac{\partial \dot{x}_7}{\partial x_5} & \frac{\partial \dot{x}_7}{\partial x_6} & \frac{\partial \dot{x}_7}{\partial x_7} \end{bmatrix}$$

where  $\underline{x}$  and  $\dot{\underline{x}}$  are the state vector and its rate of change.  $F$  is evaluated by assuming  $\underline{x}$  equals  $\hat{\underline{x}}$ , the current state estimate.

From  $F$  it computes a state transition matrix, ignoring changes in  $F$  over the integration step:

$$[2] \quad \phi \approx \mathbf{1} + \Delta t F + \frac{1}{2}(\Delta t)^2 F^2$$

where

$\Delta t$ , represented in the simulation program as STEP, is the integration step;

$\phi$ , represented in the simulation program as PHI, is the state transition matrix.

It can compute the state estimate at the end of the integration step by second-order Runge-Kutta integration:

$$[3] \quad \underline{k}_1 = \left( \hat{\underline{q}} \odot \left[ \frac{\frac{1}{2} \mathbf{I}^{-1} \mathbf{A}_t(\hat{\underline{q}}) \hat{\underline{L}}}{0} \right] \right) \Delta t$$

$$[4] \quad \underline{q}_t = (\hat{\underline{q}} + \underline{k}_1) / (|\hat{\underline{q}} + \underline{k}_1|)$$

$$[5] \quad \underline{k}_2 = \hat{\underline{q}} \odot \left[ \frac{\frac{1}{2} \mathbf{I}^{-1} \mathbf{A}_t(\underline{q}_t) \hat{\underline{L}} \Delta t}{0} \right]$$

$$[6] \quad \hat{\underline{x}} \leftarrow \left[ \frac{\hat{\underline{q}} + \frac{1}{2}(\underline{k}_1 + \underline{k}_2) / (|\hat{\underline{q}} + \frac{1}{2}(\underline{k}_1 + \underline{k}_2)|)}{\hat{\underline{L}}} \right]$$

where

$\hat{\underline{q}}$ , represented in the program as the first four elements of ESTA, is the quaternion portion of the state estimate vector;

$\hat{\underline{L}}$ , represented in the program as the last three elements of ESTA, is the estimated target angular momentum;

$\hat{\underline{x}}$ , represented in the program as ESTA, is the full state estimate;

$\underline{I}^{-1}$ , represented in the program as ININV, is the inverse of the target moment-of-inertia tensor, which is assumed known;

$\Delta t$  is, again, the integration time step;

$\underline{k}_1$ ,  $\underline{q}_t$ , and  $\underline{k}_2$ , represented in the program as K1, QI, and K2, are quaternion-valued intermediate results;

$A_t(\underline{q})$  is the direction cosine matrix corresponding to quaternion  $\underline{q}$  (for any  $\underline{q}$ );

The symbol  $\odot$  denotes quaternion multiplication.

The estimate's covariance is computed from

$$[7] \quad P \leftarrow \phi P \phi^T + Q$$

where

$P$ , represented in the program as PA, is the state estimate's covariance;

$\phi$  is the state transition matrix Equation [2];

$Q$ , represented in the program as Q, is an empirical, constant, positive diagonal matrix that represents state noise, i.e., the uncertainty introduced by simplifying assumptions in the dynamics model, roundoff and other errors in numerical integration, and unmodeled torques.

ORIGINAL PAGE 15  
OF POOR QUALITY

To compute F, the program first computes the intermediate results

$$[8] \quad J = I^{-1} A_t(\underline{q})$$

where

$I^{-1}$ , represented in the program as ININV, is the inverse of the target moment of inertia tensor;

$A_t(\underline{q})$ , represented in the program as AT, is the direction cosine matrix that corresponds to the quaternion portion of the state estimate ESTA.

The program then computes

$$[9] \quad C = \begin{bmatrix} q_4 & -q_3 & q_2 \\ q_3 & q_4 & -q_1 \\ -q_2 & q_1 & q_4 \\ -q_1 & -q_2 & -q_3 \end{bmatrix}$$

$$[10] \quad D_1 = \begin{bmatrix} q_1 & q_2 & q_3 \\ q_2 & -q_1 & q_4 \\ q_3 & -q_4 & -q_1 \end{bmatrix}$$

$$[11] \quad D_2 = \begin{bmatrix} -q_2 & q_1 & -q_4 \\ q_1 & q_2 & q_3 \\ q_4 & q_3 & -q_2 \end{bmatrix}$$

$$[12] \quad D_3 = \begin{bmatrix} -q_3 & q_4 & q_1 \\ -q_4 & -q_3 & q_2 \\ q_1 & q_2 & q_3 \end{bmatrix}$$

ORIGINAL PAGE IS  
OF POOR QUALITY

$$[13] \quad D_4 = \begin{bmatrix} q_4 & q_3 & -q_2 \\ -q_3 & q_4 & q_1 \\ q_2 & -q_1 & q_4 \end{bmatrix}$$

$$[14] \quad B = CI^{-1}$$

$$[15] \quad \underline{\omega} = J\hat{L}$$

$$[16] \quad \Omega = \begin{bmatrix} 0 & \omega_3 & -\omega_2 & \omega_1 \\ -\omega_3 & 0 & \omega_1 & \omega_2 \\ \omega_2 & -\omega_1 & 0 & \omega_3 \\ -\omega_1 & -\omega_2 & -\omega_3 & 0 \end{bmatrix}$$

$$[17] \quad \underline{W}_i = BD_i\hat{L} \text{ for } i = 1, 2, 3, 4$$

where

$\underline{\omega}$ , represented in the program as twice the variable HAV (to reduce computation), is the estimated angular velocity of the target;

$\hat{L}$ , represented in the program as the last three elements of ESTA, is the angular momentum portion of the state estimate ESTA;

$q_i$  are elements of  $q$ ;

Other quantities are intermediate results or are as in previous equations.

The F matrix is assembled from these intermediate results:

$$[18] \quad F = \left[ \begin{array}{c|c|c|c|c} [W_1] & [W_2] & [W_3] & [W_4] & + \frac{1}{2}\Omega \\ \hline 0_{3 \times 4} & \frac{1}{2}q \odot \begin{bmatrix} j_1 \\ 0 \end{bmatrix} & \frac{1}{2}q \odot \begin{bmatrix} j_2 \\ 0 \end{bmatrix} & \frac{1}{2}q \odot \begin{bmatrix} j_3 \\ 0 \end{bmatrix} & \end{array} \right]$$

where  $j_i$  represents column  $i$  of the matrix  $J$ , and the other symbols are as previously defined.

These calculations are done in subroutine PRPESA.

### 3. Filter Update

Each time the guidance system receives a new image interpretation, it updates the state estimate. The formulas used are based on the normal extended Kalman filter equations, except for one small change: normally linearization would be about the current estimated state. In this filter, however, a coordinate transformation is done first: the state estimate and covariance matrix are transformed into the (currently estimated) target body coordinate system. This approach was adopted in an attempt to minimize the effects of nonlinearities. After the state estimate and covariance matrix are updated, they are converted back to the primary coordinate system.

The formulas used are best presented procedurally:

First compute  $R$ , an empirical positive diagonal matrix that represents the measurement noise covariance. This calculation, done in subroutine ATMCOV, is based on a formula derived from fitting a curve to experimental data:



[19]  $R = \text{diag} [v \ v \ v \ v/100]$

ORIGINAL PAGE IS  
OF POOR QUALITY

where

[20]  $v = 1.129 \times 10^{-9} |\underline{x}| + 0.0001$

Second, compute

[21] 
$$P^* = \begin{bmatrix} T^T P_{11} T & | & T^T P_{12} \\ \hline (T^T P_{12})^T & | & P_{22} \end{bmatrix}$$

where

T, represented in the program as T, is a transformation matrix formed from the elements of the quaternion portion of the state estimate ESTA:

[22] 
$$T = \begin{bmatrix} q_4 & -q_3 & q_2 & q_1 \\ q_3 & q_4 & -q_1 & q_2 \\ -q_2 & q_1 & q_4 & q_3 \\ -q_1 & -q_2 & -q_3 & q_4 \end{bmatrix}$$

P\*, represented in the program as PA, is the transformed covariance matrix;

P<sub>ij</sub> are submatrices of P, which is partitioned between the fourth and fifth rows and between the fourth and fifth columns.

The program uses the array PA for both P and P\* to save space, because P and P\* are never needed simultaneously and because a portion of P does not change in the transformation to P\*.

Third, calculate the Kalman gain matrix K, represented in the program as K:

ORIGINAL PAGE 13  
OF POOR QUALITY

$$[23] \quad K = P^* G^T (R + G P^* G^T)^{-1}$$

In implementing this equation in the program, it was not necessary to explicitly multiply by the sensitivity matrix G, because it has the value

$$[24] \quad G = \begin{bmatrix} 1 & 0 & 0 & 0 & 0 & 0 & 0 \\ 0 & 1 & 0 & 0 & 0 & 0 & 0 \\ 0 & 0 & 1 & 0 & 0 & 0 & 0 \end{bmatrix}$$

and serves merely to select elements of P\*.

The state estimate and covariance are now updated with the formulas:

$$[25] \quad \underline{q}' = \begin{bmatrix} x_4 & x_3 & -x_2 & -x_1 \\ -x_3 & x_4 & x_1 & -x_2 \\ x_2 & -x_1 & x_4 & -x_3 \\ x_1 & x_2 & x_3 & x_4 \end{bmatrix} \underline{q}_{\text{meas}}$$

$$[26] \quad \underline{x}^* \leftarrow \begin{bmatrix} 0 \\ 0 \\ 0 \\ 1 \\ x_5 \\ x_6 \\ x_7 \end{bmatrix} + K \text{sign}(q_4) \underline{q}'$$

[27]  $P^* \leftarrow (1 - KG)P^*$

where, again, multiplication by  $G$  is done implicitly, and  $q_{meas}$  is the measured quaternion representing target attitude.

Finally, the state estimate and covariance are transformed back to the primary coordinate system:

[28]  $\hat{x} \leftarrow \begin{bmatrix} T \begin{bmatrix} x_1^* \\ x_2^* \\ x_3^* \\ x_4^* \end{bmatrix} \\ \hline x_5^* \\ x_6^* \\ x_7^* \end{bmatrix}$

[29]  $P \leftarrow \begin{bmatrix} TP^*_{11}T^T & | & TP^*_{12} \\ \hline (TP^*_{12})^T & | & P^*_{22} \end{bmatrix}$

where

$x_i$  and  $x_i^*$  are elements of  $\hat{x}$  and  $\hat{x}^*$ ;

$P_{ij}$  and  $P^*_{ij}$  are submatrices of  $P$  and  $P^*$ , which are partitioned as above.

These calculations are done in subroutine INCRPA.

C. POSITION FILTER CHANGED LITTLE

Two changes were made to the Kalman filter that estimates translational position and velocity:

- 1) The calculation for the measurement covariance matrix was revised to reflect the better measurements provided by a better camera and the improved image interpretation algorithm described in Section V. The new formulas also acknowledge that measurement errors in x, y, and z directions are correlated and unequal.
- 2) The covariance propagation formulas were modified to reflect less uncertainty in thruster forces. Like the measurement formulas, these formulas now acknowledge that uncertainties are not equal in each direction and that they are correlated.

1. Measurement Covariance

Subroutine ESTCOV estimates the measurement error covariance from two empirical equations, derived by fitting curves to experimental data:

$$[30] \quad V_1 = 8 \times 10^{-7}(r - 5)^4 + 0.005$$

for errors along the chase vehicle x axis (camera boresight); and

$$[31] \quad V_2 = 7.36 \times 10^{-7}(r^3) + 0.016$$

for errors along either the y or the z axis.

In these formulas r is the estimated range to the target.

The values computed from Equations [30] and [31] form the diagonal elements of the covariance matrix:

$$[32] \quad R = \begin{bmatrix} V_1 & 0 & 0 \\ 0 & V_2 & 0 \\ 0 & 0 & V_2 \end{bmatrix}$$

which is expressed in vehicle coordinates. To be useful in the filter, the matrix must be converted to the primary reference frame:

$$[33] \quad R \leftarrow A_C^T R A_C$$

where  $A_C$  is the direction cosine matrix defining the chase vehicle's attitude with respect to the primary frame.  $A_C$  is supplied by the inertial measurement unit.

## 2. Covariance Propagation

Between measurements the state estimate's accuracy degrades, because:

- 1) Initial uncertainty in velocity leads to steadily increasing uncertainty in position;
- 2) If thrusters are used, the resulting acceleration cannot be known exactly; even accelerometer measurements will contain some error;
- 3) There will be differential gravitational accelerations between the chase vehicle and the target, due to gravity gradient, even when the thrusters are not used;
- 4) Oversimplifications in the dynamics model and numerical errors (roundoff, truncation, and approximations in formulas and values of variables) cause a steady growth in estimation errors.

Subroutine PROPES explicitly models thrust uncertainty and the effect of velocity errors on future position errors. The remaining error sources are accounted for by adding a small, positive, constant, diagonal matrix to the covariance matrix during propagation.

D. NEWTON-RALPHSON ITERATION IMPROVES IMAGE INTERPRETATION

The original image-interpretation algorithm did not consider perspective effects, which become significant only at close range. During this contract phase, we added a subroutine (MPROVE) that accounts for perspective effects. This subroutine improves the interpretation accuracy and decreases correlation between errors in target attitude measurements and errors in chase vehicle position measurements.

The principle behind this routine is the Newton-Ralphson method for solving systems of nonlinear equations. This method starts with an initial guess, which is the interpretation provided by the original algorithm, and successively refines it.

The first three elements of the initial guess,  $\hat{x}$ , are the x, y, and z components of the chase vehicle's position, expressed in the primary reference frame used for navigation. The remaining three elements are the first three elements of a quaternion that expresses the difference between the target spacecraft's attitude and some reference attitude. In the program, the reference attitude is taken to be the measured attitude, so this quaternion is the identity quaternion, and the first three elements are zero. The use of only three elements for the quaternions relies on the fact that a quaternion can be premultiplied by -1.0 if necessary to guarantee that its fourth element is positive. Therefore, it can be reconstructed from the other three elements with no ambiguity, because, by convention, all the quaternions have magnitudes of 1.0, and the sign of the missing element is now known.

The routine is given a measurement vector in which the first three elements are the horizontal image-plane coordinates of the three docking aid lamps. The remaining three vector elements are the vertical coordinates for these lamps.

If near-linear equations relate small changes in the viewing position and target attitude to changes in lamp image coordinates,

$$[34] \quad (\underline{v}_{\text{meas}} - \underline{v}_{\text{pred}}) = H(\underline{x} - \underline{\hat{x}})$$

where

$\underline{v}_{\text{meas}}$  is the measurement vector described previously;

$\underline{x}$  is the true position/attitude vector (with the quaternion portion expressing the error in the quaternion portion of  $\underline{\hat{x}}$ );

$\underline{v}_{\text{pred}}$  is a measurement vector predicted from  $\underline{\hat{x}}$ ;

$\underline{\hat{x}}$  is the initial guess at  $\underline{x}$ , derived from the original image-interpretation algorithm;

H is the matrix defining the near-linear relationship between changes in  $\underline{x}$  and changes in  $\underline{v}$ .

Iterations based on this approximation converge to the true solution if the initial guess is close enough to the solution so that  $(\underline{x} - \underline{\hat{x}})$  and  $(\underline{v}_{\text{meas}} - \underline{v}_{\text{pred}})$  are small quantities. The matrix H is a matrix of partial derivatives:

$$[35] \quad H = \begin{bmatrix} \frac{\partial v_1}{\partial x_1} & \frac{\partial v_1}{\partial x_2} & \dots & \frac{\partial v_1}{\partial x_6} \\ \frac{\partial v_2}{\partial x_1} & \frac{\partial v_2}{\partial x_2} & & \frac{\partial v_2}{\partial x_6} \\ \cdot & \cdot & \cdot & \cdot \\ \frac{\partial v_6}{\partial x_1} & \frac{\partial v_6}{\partial x_2} & \dots & \frac{\partial v_6}{\partial x_6} \end{bmatrix}$$

The first three rows of H represent the sensitivity of the horizontal components of the three lamps' image-plane coordinates to changes in the position/attitude vector. Each of these rows can be computed from the same formula by changing the value of  $\underline{h}_t$ , the lamp's position in the target reference frame, to represent each lamp in turn. The expression for these rows is:

$$[36] \quad \begin{bmatrix} -r_2 \\ r_1 \end{bmatrix} \begin{bmatrix} 1 & 0 \\ 0 & 1 \end{bmatrix} A_c \begin{bmatrix} \mathbf{1}_{3 \times 3} \\ \vdots \\ \vdots \end{bmatrix} 2A_t^T \begin{bmatrix} 0 & -h_{t3} & h_{t2} \\ h_{t3} & 0 & -h_{t1} \\ -h_{t2} & h_{t1} & 0 \end{bmatrix} \frac{f}{r_1}$$

in which

$\underline{r}$  is the lamp's position in the camera's reference frame, computed from

$$[37] \quad \underline{r} = \left( A_c \left( A_t^T \underline{h}_t - \begin{bmatrix} x_1 \\ x_2 \\ x_3 \end{bmatrix} \right) \right) - \underline{h}_c$$

$\underline{h}_t$  is the lamp's position in the target reference frame;

$A_c$  and  $A_t$  are direction cosine matrices that specify chase-vehicle and target attitude with respect to the primary frame used for navigation;

$\underline{x}$  is the position/attitude vector described previously;

$\underline{h}_c$  is the camera's position in the chase-vehicle frame;



$f$  is the lens focal length;

$\mathbf{1}_{3 \times 3}$  is the  $3 \times 3$  identity matrix.

For quantities that are unknown ( $A_t, \underline{x}$ ), the measured value provided by the original image-interpretation algorithm is used. The state estimate from the Kalman filter could be used for this purpose, but use of the measurements allows the system to be self-starting.

Furthermore, it simplifies the repeated use of subroutine MPROVE for successively refining the interpretation. Each time the subroutine is reexecuted, it starts with the interpretation it produced the previous time. Because it reduces the interpretation error by approximately a factor of 10 each time it is executed, it can make the error insignificant in two executions. (The errors caused by camera noise cannot be removed by any interpretation scheme. They can only be averaged out by taking multiple measurements. This is the function of the Kalman filters, not of subroutine MPROVE.) The procedure calculates the last three rows of  $H$  from a formula almost identical to Equation [36]. These rows correspond to the sensitivity of the vertical components of the lamp-image coordinates to changes in  $\underline{x}$ . They are calculated from:

$$[38] \quad \begin{bmatrix} \frac{r_3}{r_1} & 0 & -1 \end{bmatrix} A_c \left[ \begin{array}{c} | \\ \mathbf{1}_{3 \times 3} \\ | \end{array} \right] 2A_t^T \begin{bmatrix} 0 & -h_{t_3} & h_{t_2} \\ h_{t_3} & 0 & -h_{t_1} \\ -h_{t_2} & h_{t_1} & 0 \end{bmatrix} \frac{f}{r_1}$$

Because a major portion of the calculation is the same for Equations [36] and [38], they are merged in the procedure to minimize the arithmetic. After calculating  $H$ , the procedure solves Equation [34] for  $(\underline{x} - \hat{\underline{x}})$ , the difference between the refined estimate and the initial guess. This error is added to the initial guess. However, the quaternion portion of  $\underline{x}$  expresses the error in the measured quaternion; it

does not represent attitude with respect to the primary reference frame. To get the attitude with respect to this frame, the procedure multiplies the error quaternion by the measured quaternion.

# Goal-Selection Strategy Changes



## VI. GOAL-SELECTION STRATEGY CHANGES

A simple control system has no need for goal-selection logic. It simply tries to minimize the error between the commanded position and the current position. Its control law may include some form of anticipation of the future (e.g., a phase-lead network) or other compensation to stabilize the control loop or improve performance, but it does not have to think very much to perform satisfactorily.

Such a control system is not suitable for a video rendezvous guidance system that operates with tumbling target spacecraft. The guidance system must reduce the position error to zero, but it also must do so without endangering itself or the target. This means that it must reason about avoiding a path that goes through the target. It must also avoid getting too close to the target when its knowledge of its position may be in error, and make allowance for the finite size of both the target and the chase vehicle so that the two spacecraft do not bump into each other at the side or rear end. Furthermore, it must try to keep the docking aid within the field of view of the television camera and, if possible, minimize fuel use.

The goal-selection logic implemented in the simulation program attempts to do all these things. To minimize the complexity of the task, we have divided the problem into two nearly independent subproblems, attitude and position control.

### A. ATTITUDE GOAL SELECTION

Attitude control is by far the simpler of the two problems. The logic for attitude goal selection is in subroutine RPY, which replaces two subroutines (ESTRPY and RPY) of the original program. The original routines used the state estimate from the Kalman filter only when direct video imagery was unavailable. In contrast, the new routine always uses the state estimate and never uses the video image data directly. This is possible because the filter now provides target attitude information as well as position data.

The strategy of the subroutine is simple: it adjusts yaw and pitch angles to keep the chase vehicle's docking fixture pointed directly at the end of the target's docking fixture, and it adjusts the roll angle to align the camera with the docking aid lights.

It allows for target motion by predicting the target's attitude and the chase vehicle's position at the end of the sample interval, 1.2333 s into the future. This anticipation reduces errors by compensating for control system lag.

1. The Logic of RPY

Subroutine RPY first propagates the state estimates for position and target attitude 1.2333 s into the future so that all planning is based on where things will be at the end of the decision interval, not on where they are at the start of the interval. Because movement in this time interval will be small, the subroutine uses simple Euler numerical integration of the state estimates with the assumption that all thrusters are off.

It then computes the vector from the chase vehicle center of mass (at its assumed new position) to the tip of the target's docking fixture (at its assumed new position). This vector is expressed in the chase vehicle's coordinate system:

$$[39] \quad \underline{p} = A_c (A_t^T \underline{h}_{dt} - \underline{r})$$

where

$A_c$  and  $A_t$  are direction cosine matrices that describe the attitudes of the chase vehicle and the target;

$\underline{h}_{dt}$  is the position of the docking fixture tip in the target's body coordinate system;

$\underline{\hat{x}}$  is the estimated chase vehicle position.

The subroutine then estimates yaw and pitch errors from arc tangents of the ratios of the elements of  $\underline{p}$ :

$$[40] \quad (\text{yaw error}) = \tan^{-1} \left( \frac{-p_2}{p_1} \right)$$

$$[41] \quad (\text{pitch error}) = \tan^{-1} \left( \frac{p_3}{p_1} \right)$$

The roll error is found by calculating a unit vector  $\underline{r}$  that is parallel to the target "-y" axis. This vector is expressed in the chase vehicle's body coordinate system. Then,

$$[42] \quad (\text{roll error}) = \tan^{-1} \left( \frac{-r_3}{r_2} \right)$$

#### B. TRANSLATIONAL POSITION GOAL SELECTION

The logic of subroutine SETGOL selects a translational position goal. It starts by predicting the target's attitude, but it predicts farther into the future than the end of the decision interval, because the chase vehicle may take several minutes to reach the target. The number of seconds of anticipation is an empirically chosen function of range.

We found that bad performance resulted from too much anticipation: the chase vehicle did not match the docking fixture's tangential velocity component well. Too little anticipation was also bad: the chase vehicle lagged behind the docking fixture, resulting in poor alignment. The empirical formula that seemed to give best overall results allowed 0.2 s anticipation for each meter of range, with a maximum anticipation of 20 s.

Because nonlinearities could be significant in propagating attitude for 20 s, we used second-order Runge-Kutta numerical integration rather than the much simpler Euler integration. However, no perceptible performance improvement results from this, because significant errors occur only at a considerable distance from the target.

After predicting target attitude, the subroutine selects a goal on the chase vehicle's docking axis. The distance between the goal and the target is at least enough to accommodate the docking fixtures of the two spacecraft. Under certain circumstances, however, an additional safety margin is allowed.

First, at distances over 12 m from the target, the subroutine allows for a safety margin of twice the standard deviation associated with its state estimate, or approximately three times the probable error in its knowledge of its position. The accuracy information it needs to compute this margin is taken from the diagonal elements of the covariance matrix maintained by the Kalman filter.

Second, the subroutine allows additional margin for misalignment between the two spacecraft. For example, if the chase vehicle is in the right position but the wrong attitude, it might damage the target with its solar panels. The allowance for misalignment varies from zero to 19.5 m, depending on the amount of misalignment.

Third, subroutine MODGOL analyzes the path from the current position to the goal. If it finds that the goal is on the far side of the target and that the path passes too close to the target, it revises the goal. The new goal it selects is on the shortest circular path around the target at a safe distance.





# Appendix



## APPENDIX A--PROGRAM LISTING

---

The program listing in this appendix is provided to document the simulation methods used in analyzing the three-light video guidance system and running the simulation. It was written to run on a Prime 550 computer under the PRIMOS operating system, but it has few hardware-dependent subroutines. If it is to be run on another computer, the following information will prove useful.

Several library routines are used, and these are not shown in the listing. The routines include ASIN and ACOS, which compute the inverse trigonometric functions arc sine and arc cosine. The function RANFN is a random number generator that computes normally distributed random values with a specified mean and standard deviation. In addition, the matrix arithmetic routines MADD (addition), MSJB (subtraction), MMLT (multiplication), MINV (matrix inversion), MSCL (multiplication by a scalar), MIDN (setting an array equal to the identity matrix), and MTRN (forming the transpose of a matrix) are used from the Prime library MATHLB.

File handling may present conversion problems even if the program is to be run on another Prime 550 computer, because logical unit numbers, file names, and amount of disk storage vary from installation to installation. Standard Prime subroutines are used to open and close files. These subroutines (TSRC\$\$, EXST\$A, CLOS\$A, and DELE\$A) are from the Prime library APPLIB.

Run time is approximately twice real time if the computer is dedicated to one user.

The perspective drawings shown in this report are not created directly by this program. They are drawn by a second program that uses the data file created by this program. This allows the creation of stereo plots and views from different perspectives.

Several WRITE statements in subroutine DOCK are rendered inactive by a character C in the first column of text. Removing this character will provide a printout at the operator's terminal for monitoring the progress of the simulation;

The first part of the listing is the text of a terminal session, which includes compilation, loading, and execution of the program.

ORIGINAL PARTS  
OF POOR QUALITY

```

ENTER PATHNAME FOR OUTPUT
DK, CD, C, PHASE3A -DCLVAR
***FILE ALREADY EXISTS DK TO OVERWRITE? YES
ENTER THREE ROTATION ANGLES TO SPECIFY INITIAL TARGET
ATTITUDE FOR A YAW-PITCH-ROLL SEQUENCE---ANGLES MUST BE
IN DEGREES
0
0
ENTER TUMBLE AXIS-- ENTER 1, 2, OR 3 FOR YAW, PITCH,
OR ROLL, RESPECTIVELY
1
ENTER TUMBLE RATE IN DEGREES PER HOUR
900
INPUT 16-DIGIT RANDOM INTEGER
529639470960370954334
DO YOU WANT ANOTHER SIMULATION? NO

DK, FTN, RES, C, PHASE3A
0000 ERRORS L<MAIN>FTN-REV17 43
0000 ERRORS L<OPEN>FTN-REV17 43
0000 ERRORS L<INIPAR>FTN-REV17 43
0000 ERRORS L<INLSIN>FTN-REV17 43
0000 ERRORS L<DOCK>FTN-REV17 43
0000 ERRORS L<PROBT>FTN-REV17 43
0000 ERRORS L<CCMPK1>FTN-REV17 43
0000 ERRORS L<CCMPK2>FTN-REV17 43
0000 ERRORS L<CCMPK3>FTN-REV17 43
0000 ERRORS L<CCMPK4>FTN-REV17 43
0000 ERRORS L<DOIT>FTN-REV17 43
0000 ERRORS L<ATLUD>FTN-REV17 43
0000 ERRORS L<FINDCV>FTN-REV17 43
0000 ERRORS L<GUATRIN>FTN-REV17 43
0000 ERRORS L<INCORP>FTN-REV17 43
0000 ERRORS L<CCMPG>FTN-REV17 43
0000 ERRORS L<LUCAN>FTN-REV17 43
0000 ERRORS L<LUPDST>FTN-REV17 43
0000 ERRORS L<LUPDCV>FTN-REV17 43
0000 ERRORS L<PROPS>FTN-REV17 43
0000 ERRORS L<SETGOL>FTN-REV17 43
0000 ERRORS L<MODGOL>FTN-REV17 43
0000 ERRORS L<CONLAN>FTN-REV17 43
0000 ERRORS L<ACCEL1>FTN-REV17 43
0000 ERRORS L<SELECT>FTN-REV17 43
0000 ERRORS L<TABLE1>FTN-REV17 43
0000 ERRORS L<ABES>FTN-REV17 43
0000 ERRORS L<LUM>FTN-REV17 43
0000 ERRORS L<IRPY>FTN-REV17 43
0000 ERRORS L<IMPROVE>FTN-REV17 43
0000 ERRORS L<MINV6>FTN-REV17 43
0000 ERRORS L<TORQUA>FTN-REV17 43
0000 ERRORS L<LUCAN>FTN-REV17 43
0000 ERRORS L<CCMP1>FTN-REV17 43
0000 ERRORS L<CCMP2>FTN-REV17 43
0000 ERRORS L<ATMCOV>FTN-REV17 43
0000 ERRORS L<PRPES4>FTN-REV17 43
0000 ERRORS L<CMPCD>FTN-REV17 43
0000 ERRORS L<DDCHK>FTN-REV17 43
0000 ERRORS L<STRAT>FTN-REV17 43
0000 ERRORS L<FORCE>FTN-REV17 43
0000 ERRORS L<IMPRIME>FTN-REV17 43
0000 ERRORS L<LIMAC>FTN-REV17 43
0000 ERRORS L<TORQUE>FTN-REV17 43
0000 ERRORS L<LAPME>FTN-REV17 43
0000 ERRORS L<CPRTM>FTN-REV17 43
0000 ERRORS L<SGRI>FTN-REV17 43
0000 ERRORS L<LANGVE>FTN-REV17 43
0000 ERRORS L<STRCAT>FTN-REV17 43
0000 ERRORS L<GMLT>FTN-REV17 43
0000 ERRORS L<DPRD>FTN-REV17 43

DK, LOAD
$ LO, B, MSFC, PHASE3A
$ LO, T, TIEZ, WORKING, NERD, B, ASIN
$ LI, APPLIB
$ LI, PATHL
LOAD COMPLETE
$ SA, *PHASE3A
$ BU

DK, CU, TTY
DK, R, *PHASE3A

```







```

C      (* INPUT INITIAL ATTITUDE ANGLES *)
C      READ(TERML,904) PAI,PSI,THETA
C      (* CONVERT ANGLES TO RADIAN *)
C      PHI=PI*01745329
C      PSI=PSI*01745329
C      THETA=THETA*01745329
C      (* COMPUTE TRANSPOSE OF TRUE INITIAL TARGET ATTITUDE *)
C      TRMAT(1,1)=COS(PSI)*COS(PHI)
C      TRMAT(1,2)=SIN(PSI)*COS(PHI)
C      TRMAT(1,3)=SIN(PSI)*SIN(PHI)
C      TRMAT(2,1)=-SIN(THETA)*SIN(PSI)*COS(PHI)-COS(THETA)*SIN(PHI)
C      TRMAT(2,2)=SIN(THETA)*SIN(PSI)*COS(PHI)+COS(THETA)*SIN(PHI)
C      TRMAT(2,3)=SIN(THETA)*SIN(PSI)*SIN(PHI)+COS(THETA)*SIN(PHI)
C      TRMAT(3,1)=SIN(THETA)*COS(PSI)
C      TRMAT(3,2)=SIN(THETA)*SIN(PSI)
C      TRMAT(3,3)=COS(THETA)*COS(PSI)
C      (* INPUT TUMBL AXIS *)
C      WRITE(TERML,902)
C      READ(TERML,*) ITUMBL
C      IF(ITUMBL EQ 1 OR ITUMBL EQ 2 OR ITUMBL EQ 3) GO TO 5
C      GO TO 3
C      (* INPUT TUMBLE RATE *)
C      WRITE(TERML,903)
C      READ(TERML,*) TUMRAT
C      (* CONVERT TUMBLE RATE FROM DEGREES/HOUR TO RADIAN/SECOND *)
C      TUMRAT=TUMRAT*848137E-6
C      A=1
C      B=1
C      DDMR=4
C      FDCLEN=5
C      F1(1)=360
C      F1(2)=160
C      F1(3)=160
C      F1(4)=160
C      F1(5)=160
C      F1(6)=160
C      F1(7)=160
C      F1(8)=160
C      F1(9)=160
C      F1(10)=160
C      F1(11)=160
C      F1(12)=160
C      F1(13)=160
C      F1(14)=360
C      DO 10 I=1,3
C      DO 10 J=1,3
C      INERC(I,J)=0
C      INERC(1,1)=1055
C      INERC(1,2)=1905
C      INERC(1,3)=1905
C      INERC(2,1)=1905
C      INERC(2,2)=1905
C      INERC(2,3)=1905
C      INERC(3,1)=1905
C      INERC(3,2)=1905
C      INERC(3,3)=1905
C      TPHIV=5
C      T=0
C      DO 20 I=1,14
C      DO 20 J=1,3
C      CONTINUE=1.3
C      DO 30 DO 30 J=1,3
C      DO 30 FULDIS(I,J)=0
C      CONTINUE
C      FULDIS(1,1)=781
C      FULDIS(1,2)=706
C      FULDIS(1,3)=706
C      DO 40 I=1,14
C      DO 40 AK(I)=4.636E-4
C      CONTINUE
C      DO 50 I=1,3
C      DO 50 J=1,14
C      AK2(I,J)=0
C      AK3(I,J)=0
C      ANS(I,J)=0
50 CONTINUE
C      ANS(2,1)=1
C      ANS(2,2)=1
C      ANS(2,3)=1
C      AK2(2,4)=1
C      AK2(2,5)=1
C      AK2(2,6)=1
C      AK2(2,7)=1
C      ANS(2,8)=1
C      ANS(2,9)=1
C      AK2(3,10)=1
C      AK2(3,11)=1
C      AK2(3,12)=1
C      AK2(3,13)=1
C      ANS(1,14)=1
C      AK3(3,1)=75
C      AK3(3,2)=75
C      AK3(3,3)=75
C      AK3(3,4)=75
C      AK3(1,5)=75
C      AK3(1,6)=75
C      AK3(1,7)=75
C      AK3(1,8)=75
C      AK3(1,9)=75
C      AK3(1,10)=75
C      AK3(2,11)=75
C      AK3(2,12)=75
C      AK3(2,13)=75
C      MEMPTV=1800
C      DO 60 I=1,6
C      DO 60 J=1,6
60 CONTINUE
C      CALL MIDN(INV,3)
C      CALL MIDN(PA,7)
C      P(1,1)=400
C      P(2,2)=363
C      P(3,3)=363
C      P(4,4)=03
C      P(5,5)=03
C      P(6,6)=03
C      ESTATE(1)=-300
C      ESTATE(2)=0
C      ESTATE(3)=0
C      ESTATE(4)=1
C      ESTATE(5)=1
C      ESTATE(6)=1
C      ININV(1,1)=4.5E-5
C      ININV(2,2)=3.56E-5
C      ININV(3,3)=3.56E-5
C      ESTA(1)=0
C      ESTA(2)=0
C      ESTA(3)=0
C      ESTA(4)=0
C      ESTA(5)=0
C      ESTA(6)=0
C      ESTA(7)=0
C      PA(1,1)=10
C      PA(2,2)=10
C      PA(3,3)=10
C      PA(4,4)=10
C      PA(5,5)=4.E6
C      PA(6,6)=4.E6
C      PA(7,7)=4.E6
C      DO 70 I=1,6
C      DO 70 J=1,6
70 STATE(I)=RANFN(2,ESTATE(I),SQRT(P(I,I)))
C      CONTINUE=0
C      STATE(8)=0
C      STATE(9)=0
C      STATE(10)=0
C      STATE(11)=0
C      STATE(12)=0
C      STATE(13)=1700
C      GO(1)=STATE(10)

```





ORIGINAL PAGE IS  
OF POOR QUALITY

COMMON/OPTSYS/TPH14.TPH1V.FOCLN.DUMMY4(2)

```

SUBROUTINE DOCK(P,ESTATE,STATE,T,DOCKED,F,ESTA,PA)
(* 400 - RUN SIMULATION FOR ONE MEASUREMENT INTERVAL *)
CALLS TOOL, INCORP, SORT, FLASH, PROPT, POSIT, ATTUD, PROPS, THRUST,
      TRM, RPY, MELT, MSUB, HADD, MPROVE, INCRPA, PRPRES, AMAXI, DOKCHK, DPRD
      CALLED BY
      CHAIN)
INPUT ESTATE, DOKRAD, STATE, T, F, INERCV
OUTPUT ESTATE, T, F, DOCKED, ESTATE, P
REAL ACV(3,3), ACVT(3,3)
      DIRECTION COSINE MATRIX DESCRIBING CURRENT CHASE VEHICLE ATTITUDE
      RELATIVE TO PRIMARY REFERENCE FRAME) AND TRANSPOSE OF ACV
      MEASURED(3)
      DIRECTION COSINE MATRIX OF TARGET SPACECRAFT
      MEASURED ATTITUDE RATES ABOUT CHASE VEHICLE AXES
      MEASURED CHASE VEHICLE POSITION IN PRIMARY REFERENCE FRAME
      TIME IN WHICH STRATEGY LOGIC WANTS CHASE VEHICLE IN GOAL 'BOX'
      RADIUS FROM TARGET AT WHICH CHASE VEHICLE IS CONSIDERED DOCKED
      CHANGE IN CENTER-LAMP IMAGE COORDINATES BETWEEN FLASHES
      ESTIMATE FOR TARGET ATTITUDE
      STATE VECTOR FOR CHASE VEHICLE TRANSLATION
      ESTIMATE OF STATE VECTOR FOR CHASE VEHICLE AFTER SELECTION
      FORCES FROM CHASE VEHICLE THRUSTERS AFTER SELECTION
      LOCAL LENGTH (MM)
      LOCAL COORDINATE SYSTEM
      UPPER-LOWER LIMITS OF GOAL 'BOX'
      DOCKING FIXTURES' POSITIONS IN RESPECTIVE SPACECRAFT COORDINATE
      SYSTEMS
      INTEGER UNIT NUMBER FOR OUTPUT FILE
      PROGRAM PA(7,7)
      COVARIANCE OF STATE ESTIMATES CORRESPONDING TO ESTATE(1) AND ESTA(1)
      MEAS(4)
      MEASURED TARGET ATTITUDE QUATERNION (W R T PRIMARY FRAME)
      RELATIVE CAMERA COORDINATES IN CURRENT DOCKING AID FRAME CENTERED
      AT CENTER LIGHT
      MEASURED RANGE, CAMERA TO TARGET DOCKING AID CENTER LIGHT
      MEASURD ROLL, PITCH, AND YAW ERRORS IN RADIANS
      CHASE VEHICLE STATE VECTOR
      ELAPSED TIME
      TRANSPOSE OF TARGET SPACECRAFT DIRECTION COSINE MATRIX
      (WITH RESPECT TO TRUTH AXES) FOR OUTPUT ONLY
      TRM, TPH1V
      HALF-FIELD-OF-VIEW ANGLES FOR HORIZ, VERT
      COORDINATES OF LAMPS' IMAGES
      LOGICAL DOCKED
      LOGICAL VALID
      TRUE IF MEASUREMENT VALID (LIGHT IN FIELD OF VIEW)
      TRUE IF MEASUREMENT VALID (LIGHT IN FIELD OF VIEW)
COMMON/SIMUL/DUMMY, OUT
COMMON/HNOFF/DUMMY3(6), HOC, HDT
COMMON/VEHIC/DUMMY1(98), DOKRAD, DUMMY2(14)

```

```

C      (* TAKE MEASUREMENT *)
C      VAL(1) = FLASH CENTER LIGHT *
C      (* 410 - FLASH CENTER LIGHT *)
C      CALL FLASH(U(4), V(4), 2, T, STATE, VALID)
C      (* 420 - PROPAGATE TRUE STATE 1/30 SEC *)
C      CALL PROPTR(0333333, F, STATE, T)
C      (* 410 - FLASH LEFT LIGHT *)
C      CALL FLASH(U(1), V(1), 1, T, STATE, VALID)
C      (* 420 - PROPAGATE TRUE STATE 1/30 SEC *)
C      CALL PROPTR(0333333, F, STATE, T)
C      (* 410 - FLASH RIGHT LIGHT *)
C      CALL FLASH(U(3), V(3), 3, T, STATE, VALID)
C      (* 420 - PROPAGATE TRUE STATE 1/30 SEC *)
C      CALL PROPTR(0333333, F, STATE, T)
C      (* 410 - FLASH RIGHT LIGHT *)
C      CALL FLASH(U(2), V(2), 2, T, STATE, VALID)
C      (* 420 - PROPAGATE TRUE STATE 1/30 SEC *)
C      CALL PROPTR(0333333, F, STATE, T)
C      (* 420 - PROPAGATE TRUE STATE TO TIME OF THRUSTER COMMAND CHANGE *)
C      CALL PROPTR(0333333, F, STATE, T)
C      (* 430 - POSITIONS AT TIME OF THRUSTER COMMAND CHANGE *)
C      CALL PROPTR(0333333, F, STATE, T)
C      (* 440 - CALC TARGET ATTITUDE AND CHASE VEHICLE POSITION AT 4TH FLASH *)
C      CALL ATITUD(ACV, ACVT, RELPOS, RMO, U, V, GREAS, CUPOS)
C      (* 450 - REFINE INHERENT POSITION TO ACCOUNT FOR PERSPECTIVE *)
C      CALL IMPROVE(U, V, ACV, GREAS, CUPOS)
C      (* 460 - USE MEASUREMENT TO UPDATE STATE ESTIMATE *)
C      CALL INCORP(CUPOS, P, ESTATE, ACV, ACVT)
C      (* 470 - USE MEASUREMENT TO UPDATE ATTITUDE STATE ESTIMATE *)
C      CALL INCRPA(ESTATE, ESTATE, GREAS)
C      (* 480 - CALC LATEST IMU READING *)
C      CALL IMU(STATE, ACV, ACVT, ATRATE)
C      (* 490 - CALCULATE ROLL, PITCH, YAW ERRORS *)
C      CALL RPYERR(ACV, ESTA)
C      (* 480 - COMPUTE ESTATE GIL, GYM, GYL, GYM, GYL, GYM, GYL, ANAXI)
C      CALL TMIN(T, O, ACV, ATRATE, RPYERR)
C      (* 420 - PROPAGATE TRUE STATE TO TIME OF FIRST FLASH OF NEXT SEQUENCE *)
C      CALL PROPTR(0.5, F, STATE, T)
C      (* 430 - PROP STATE ESTIMATE TO TIME OF 4TH FLASH OF NEXT SEQUENCE *)
C      CALL PROPSP(ESTATE, ESTATE, STATE)
C      (* 440 - PROP ESTATE TO STATE ESTIMATE TO SAME TIME *)
C      CALL PROPSPA(ESTATE, T)
C      (* 450 - SEE IF CHASE VEHICLE HAS DOCKED YET *)
C      CALL DOCKM(INDC, STATE, DOKRAD, HDY, DOCKED, T)
C      (* 460 - WRITE PARAMETERS TO DISK FILE *)
C      CALL TRCAT(TAOUT, T)
C      WRITE(OUT, 1, STATE, ADUT)
C      WRITE(1, 903) STATE(4), STATE(5), STATE(6)
C      WRITE(1, 904) STATE(10), STATE(11), STATE(12), STATE(13)
C      WRITE(1, 905) STATE(7), STATE(8), STATE(9)
C      WRITE(1, 905) STATE(14)
C      (* SWAP LENSES IF NECESSARY *)
C      IF (YPRIM=1) DPRED(ESTATE, ESTATE, 3) GT 225 ) GO TO 20
C      IPRIM=1
C      FOLLEN=025
C      GO TO 30
C      CONTINUE
C      IPRIM=0
C      FOLLEN=03
C      RETURN
C      901 FORMAT('-----TIMES', F10.2, ' POSITION IS ', G14.7)
C      902 FORMAT(' VELOCITY', G14.7)
C      903 FORMAT(' DECELERATION IS ', G14.7)
C      904 FORMAT(' ANGULAR MOMENTUM IS ', G14.7)
C      905 FORMAT(' MASS IS ', G14.7)
C      END

```



```

SUBROUTINE COMPA1(F,K1,STATE,STEP,T)
(* 421 - COMPUTE VECTOR K1 FOR RUNGE-KUTTA INTEGRATION *)
CALLS
CALLED BY
PROPTB
INPUT STATE, STEP, T, FULDIS, INERCV, MEMPTY
OUTPUT
K1
REAL DSTATE(14)
TIME DERIVATIVE OF STATE VECTOR
REAL F(14)
FORCES FROM THRUSTERS AFTER SELECTION
REAL FULDIS(3,3)
CHASE VEHICLE FUEL-DISTRIBUTION INERTIA TENSOR
INTEGER I
DO LOOP INDEX
REAL INERCV(3,3)
CHASE VEHICLE MOMENT OF INERTIA TENSOR
REAL FULDIS(3,3)
INERTIA OF FUEL
REAL INERTA(3,3)
INERTIA OF CHASE VEHICLE (LOADED)
REAL K1(14)
VECTOR K1 USED IN RUNGE-KUTTA INTEGRATION
REAL STATE(14)
CHASE VEHICLE MASS WITHOUT FUEL
REAL STATE(14)
CHASE VEHICLE STATE VECTOR
REAL STEP
REAL STEP SIZE FOR INTEGRATION
REAL T
ELAPSED TIME
COMMON/MASPRP/FULDIS,INERCV,MEMPTY
(* COMPUTE INERTIA *)
CALL MSCL(INERFL,FULDIS,3,3,STATE(14)-MEMPTY)
CALL MADD(LINERV,INERCV,INERFL,3,3)
(* CALL COMPUTE STATE INERTIA *)
(* COMPUTE K1=STEP*(STATE DERIVATIVE) *)
DO 10 I=1,14
K1(I)=STEP*DSTATE(I)
10 CONTINUE
RETURN
END

```

```

SUBROUTINE PROPTR(DT,F,STATE,T)
(* 420 - PROPAGATE TRUE STATE BY 4TH-ORDER RUNGE-KUTTA INTEGRATION *)
CALLS
CALLED BY
POINT, AMINI, SORT
30CA
INPUT DT, F, STATE, T
OUTPUT
STATE, T
REAL D)
INTEGRATION INTERVAL SIZE
REAL F(14)
FORCES FROM THRUSTERS AFTER SELECTION
INTEGER I
DO LOOP INDEX
REAL K1(14), K2(14), K3(14), K4(14)
VECTORS K1, K2, K3, K4 USED IN RUNGE-KUTTA INTEGRATION
REAL QM
SQUARE ROOT OF SUM OF SQUARES OF QUATERNION ELEMENTS
REAL STATE(14)
CHASE VEHICLE STATE VECTOR
REAL STEP
STEP SIZE FOR INTEGRATION
REAL T, TO
ELAPSED TIME AND TIME AT START OF INTEGRATION INTERVAL
REAL TLEFT
TIME LEFT TO GO OUT OF DT
PARAMETER STATE(14), INTEGRATION STEP SIZE
REAL TLEFT=DT
TO=T
10 IF(TLEFT LE 0) GO TO 40
STEP=AMINI*(STEP**NR, TLEFT)
(* 421 - COMPUTE K1 *)
CALL COMPA1(F, K1, STATE, STEP, T)
(* 422 - COMPUTE K2 *)
CALL COMPA2(F, K2, STATE, STEP, T, K1)
(* 423 - COMPUTE K3 *)
CALL COMPA3(F, K3, STATE, STEP, T, K1, K2)
(* 424 - COMPUTE K4 *)
CALL COMPA4(F, K4, STATE, STEP, T, K1, K2, K3)
(* COMPUTE NEW STATE *)
DO 20 I=1,14
STATE(I)=STATE(I) + K1(I)*2 + K2(I)*2 + K3(I) + K4(I))/4
20 CONTINUE
NORMALIZE QUATERNION *)
QM=STATE(14)**2
STATE(14)=SQRT(QM)
DO 30 I=1,13
STATE(I)=STATE(I)/QM
30 CONTINUE
POINT SIMULATION CAMERA *)
CALL POINT(STATE)
GO TO 10
40 CONTINUE
T=T+DT
RETURN
END

```

```

SUBROUTINE COMPK3(F,K2,STATE,STEP,I,K3)
(* 423 - DETERMINE VECTOR K3, FOR RUNGE-KUTTA INTEGRATION *)
CALLS
MADD,MSCL,STPRIM
CALLED BY
PROPTR
INPUT,FULDIS,INERCV,K2,EMPTY,STATE,STEP,I
OUTPUT
K3
REAL DSTATE(14)
TIME,DERIVATIVE OF STATE VECTOR
REAL F(14)
FORCES FROM THRUSTERS AFTER SELECTION
REAL FULDIS(3,3)
CHASE,VEHICLE FUEL-DISTRIBUTION INERTIA TENSOR
INTEGER I
DO LOOP INDEX
REAL INERCV(3,3)
INERTIA OF EMPTY CHASE VEHICLE
REAL INERFL(3,3)
INERTIA OF FUEL
REAL INERTA(3,3)
INERTIA OF CHASE VEHICLE (LOADED)
REAL K2(14),K3(14)
VECTORS K2 AND K3 USED IN RUNGE-KUTTA INTEGRATION
REAL EMPTY
MASS OF CHASE VEHICLE WITHOUT FUEL
REAL STATE(14)
CHASE,VEHICLE STATE VECTOR
REAL STEP
STEP SIZE FOR INTEGRATION
REAL T
ELAPSED TIME
REAL TEMPST(14)
TEMPORARY STATE VECTOR
COMMON/MASPRP/FULDIS,INERCV,EMPTY
(* COMPUTE TEMPORARY STATE *)
DO I=1,14
TEMPST(I)=STATE(I)+0.5*K2(I)
10 CONTINUE TEMPORARY INERTIA AS A FUNCTION OF TEMPORARY
STATE MASS *)
CALL MSCL(INERFL,FULDIS,3,3,TEMPST(14)-EMPTY)
CALL MADD(INERTA,INERCV,INERFL,3,3)
(* 902 - COMPUTE DERIVATIVE AT TEMPORARY STATE *)
CALL STPRIM(TEMPST,F,INERTA,T,5*STEP,DSTATE)
(* COMPUTE K3=STEP*DERIVATIVE AT TEMPORARY STATE *)
DO K3(I)=STEP*DSTATE(I)
20 CONTINUE
RETURN
END

```

```

SUBROUTINE COMPK2(F,K1,STATE,STEP,I,K2)
(* 422 - DETERMINE VECTOR K2, FOR RUNGE-KUTTA INTEGRATION *)
CALLS
MADD,MSCL,STPRIM
CALLED BY
PROPTR
INPUT,FULDIS,INERCV,K1,EMPTY,STATE,STEP,I
OUTPUT
K2
REAL DSTATE(14)
TIME,DERIVATIVE OF STATE VECTOR
REAL F(14)
FORCES FROM THRUSTERS AFTER SELECTION
REAL FULDIS(3,3)
CHASE,VEHICLE FUEL-DISTRIBUTION INERTIA TENSOR
INTEGER I
DO LOOP INDEX
REAL INERCV(3,3)
INERTIA OF EMPTY CHASE VEHICLE
REAL INERFL(3,3)
INERTIA OF FUEL
REAL INERTA(3,3)
INERTIA OF CHASE VEHICLE (LOADED)
REAL K1(14),K2(14)
VECTORS K1 AND K2 USED IN RUNGE-KUTTA INTEGRATION
REAL EMPTY
MASS OF CHASE VEHICLE WITHOUT FUEL
REAL STATE(14)
CHASE,VEHICLE STATE VECTOR
REAL STEP
STEP SIZE FOR INTEGRATION
REAL T
ELAPSED TIME
REAL TEMPST(14)
TEMPORARY STATE VECTOR
COMMON/MASPRP/FULDIS,INERCV,EMPTY
(* COMPUTE TEMPORARY STATE *)
DO I=1,14
TEMPST(I)=STATE(I)+0.5*K1(I)
10 CONTINUE TEMPORARY INERTIA AS FUNCTION OF TEMPORARY
STATE MASS *)
CALL MSCL(INERFL,FULDIS,3,3,TEMPST(14)-EMPTY)
CALL MADD(INERTA,INERCV,INERFL,3,3)
(* 902 - COMPUTE DERIVATIVE AT TEMPORARY STATE *)
CALL STPRIM(TEMPST,F,INERTA,T,5*STEP,DSTATE)
(* COMPUTE K2=STEP*DERIVATIVE AT TEMPORARY STATE *)
DO K2(I)=STEP*DSTATE(I)
20 CONTINUE
RETURN
END

```











```

C SUBROUTINE INCORP(CVPOD,P,ESTATE,ACV,ACVT)
C (* 450 - INCORPORATE MEASUREMENT *)
C CALLS UPDCOV,UPDSTA,COMP,G,ESTCOV,KALGAN,MINV,MSUB,MMLT
C CALLED BY DOCK
C INPUT ESTATE,P,R
C OUTPUT P,ESTATE
C REAL ACV(3,3),ACVT(3,3)
C DIRECTION COSINE MATRIX MEASURED BY IMU, GIVING CHASE VEHICLE
C REAL CVPOD(3) AND THE TRANSPOSE OF THIS MATRIX
C MEASURED CHASE VEHICLE POSITION IN PRIMARY REFERENCE FRAME
C INTEGER ERR
C ERROR CODE (=0 IF OKAY)
C ESTIMATE OF STATE VECTOR
C PARTIAL OF MEASUREMENT WITH RESPECT TO STATE
C REAL KGAIN(6,3)
C KALMAN GAIN MATRIX
C INTEGER I,J
C DO LOOP INDICES
C REAL GAIN(3,3),P(3,3),PAI(3,3)
C COMPUTE GAIN,P,ESTIMATE,ITS UPPER LEFT 3X3 SUBMATRIX, AND
C THE INVERSE OF THAT SUBMATRIX
C REAL R(3,3)
C MEASUREMENT COVARIANCE
C REAL T1(3),E(3),C,SCRACH(4,6)
C -- TEMPORARY VARIABLES
C -- (* CHECK FOR RIDICULOUS VALUE *)
C DO 10 I=1,3
C DO 20 J=1,3
C PAI(I,J)=P(I,J)
C CONTINUE
C CALL MINV(PA,PA,3,SCRACH,4,6,ERR)
C TEMPORAL G DO 10 J=1,3
C CALL MMLT(P,DOSESTATE,3,1)
C CALL MMLT(PA,E,3,1)
C CALL MMLT(C,E,T1,1,3,1)
C IF(C LE 1.60) GO TO 20
C RETURN
C 20 (* COMPUTE JACOBIAN G *)
C DO 30 I=1,3
C DO 40 J=1,3
C ESTIMATE MEASUREMENT COVARIANCE *)
C CALL ESTCOV(ESTATE,R,ACV,ACVT)
C 423 - COMPUTE KALMAN GAIN MATRIX *)
C CALL KALGAN(R,P,G,KGAIN)
C 434 - UPDATE STATE *)
C CALL UPDSTATE(ESTATE,KGAIN,CVPOD)
C CALL UPDCOV(P,KGAIN,G)
C RETURN
C 30 CONTINUE
C WRITE(1,901)
C STOP
C 901 FORMAT('P IS SINGULAR IN 'INCORP''')
C END

```

ORIGINAL PAGE IS  
OF POOR QUALITY



ORIGINAL SOURCE  
OF POOR QUALITY

```

C SUBROUTINE ESTCOV(ESTATE,R,ACV,ACVT)
C (* 432 - ESTIMATE MEASUREMENT COVARIANCE *)
C CALLS
C SQR1,DPRD,MMLT
C CALLED BY
C INCORP
C INPUT
C ESTATE
C OUTPUT
C R
C REAL ACV(3,3),ACVT(3,3)
C DIRECTION COSINE MATRIX MEASURED BY IMU, GIVING CHASE VEHICLE
C ATTITUDE AND THE TRANSPOSE OF THIS MATRIX
C REAL ESTATE(6)
C REAL ESTIMATE OF STATE VECTOR
C INTEGER I,J,INDICES
C DO LOOP
C REAL MEASUREMENT COVARIANCE
C REAL RANGE
C ESTIMATED RANGE TO TARGET SPACECRAFT
C REAL RI(3,3)
C INTERMEDIATE RESULTS
C DO I=1,3
C DO J=1,3
C DO R(J,I)=0
C RANGE=SQR1(DPRD(ESTATE,ESTATE,3))
C R(1,1)=8 E-7*(RANGE-5)**4+ 005
C R(2,2)=7 36E-7*RANGE**3+ 0016
C R(3,3)=R(2,2)/ACVT,R(3,3,3)
C CALL MMLT(R,RI,ACV,3,3,3)
C RETURN
C
C 10 CONTINUE
C R(J,I)=0
C RANGE=SQR1(DPRD(ESTATE,ESTATE,3))
C R(1,1)=8 E-7*(RANGE-5)**4+ 005
C R(2,2)=7 36E-7*RANGE**3+ 0016
C R(3,3)=R(2,2)/ACVT,R(3,3,3)
C CALL MMLT(R,RI,ACV,3,3,3)
C RETURN
C
C 20 CONTINUE
C REPORT ERROR *
C (* WRITE(TERMINL,901)
C STOP
C 901 FORMAT('MATRIX INVERSION FAILURE IN SUBROUTINE KALGAN')
C
C SUBROUTINE KALGAN(R,P,G,KGAIN)
C (* 433 - COMPUTE KALMAN GAIN MATRIX *)
C CALLS
C MADD,MINV,MMLT
C CALLED BY
C INCORP
C INPUT
C R,P,G
C OUTPUT
C KGAIN
C INTEGER I,RR
C ERROR CODE (=0 IF NO ERROR)
C REAL G(3,6)
C PARTIAL OF MEASUREMENT WITH RESPECT TO STATE
C REAL GT(5,3)
C TRANSPOSE OF G
C INTEGER I,J,INDICES
C REAL DOOP
C REAL KGAIN(6,3)
C KALMAN GAIN MATRIX
C REAL P(6,6)
C STATE ESTIMATE COVARIANCE
C REAL R(3,3)
C MEASUREMENT COVARIANCE
C REAL SCRATCHPAD
C SCRATCHPAD FOR ROUTINE MINV
C REAL TEMP1(6,3),TEMP2(3,3),TEMP3(3,3)
C INTERMEDIATE RESULTS WITH NO PROBLEM-RELATED SIGNIFICANCE
C INTEGER TERMINL
C FORTRAN UNIT NUMBER FOR TERMINAL
C COMMON/SIMUL/TERMINL,IDUMMY
C (* COMPUTE KGAIN=P*TRN(G)*INV(R+G*P*TRN(G)) *)
C DO I=1,3
C DO J=1,6
C GT(I,J)=G(I,J)
C 10 CONTINUE
C TEMP1,P,GT,6,6,3)
C CALL MMLT(TEMP2,G,TEMP1,3,6,3)
C CALL MADD(TEMP3,R,TEMP2,3,3)
C CALL MINV(TEMP2,TEMP3,3,SCRATCH,4,6,ERR)
C IF(ERR NE 0) GO TO 20
C CALL MMLT(TEMP1,GT,TEMP2,6,3,3)
C CALL MMLTKGAIN,P,TEMP1,6,6,3)
C RETURN
C 20 CONTINUE
C REPORT ERROR *
C (* WRITE(TERMINL,901)
C STOP
C 901 FORMAT('MATRIX INVERSION FAILURE IN SUBROUTINE KALGAN')
C
C

```

ORIGINAL PAGE 18  
OF POOR QUALITY

```

C SUBROUTINE UPDCOV(P,KGAIN,C)
C (* 433 - UPDATE COVARIANCE MATRIX FROM (P=(I-K*G)*P) *)
C
C CALLS
C MMLT
C CALLED BY
C INCORP
C
C INPUT
C P,KGAIN,G
C
C OUTPUT
C P
C
C REAL G(3,6) OF MEASUREMENT WITH RESPECT TO STATE
C INTEGER I,J DO LOOP INDICES
C REAL KGAIN(6,3)
C REAL KALMAN GAIN MATRIX
C REAL P(6,6)
C REAL COVARIANCE OF STATE ESTIMATE
C REAL INTERMEDIATE RESULTS WITH NO PROBLEM-RELATED SIGNIFICANCE
C
C (* COMPUTE I-KGAIN*G *)
C CALL MMLT(TEMP,KGAIN,G,3,6)
C DO I=1,6
C DO J=1,6
C TEMP(I,J)=-TEMP(I,J)
C
C 10 CONTINUE
C DO I=1,6
C TEMP(I,I)=TEMP(I,I)+1.0
C
C 20 (* COMPUTE NEW P *)
C CALL MMLT(P1,TEMP,P,6,6)
C DO I=1,6
C DO J=1,6
C P(I,J)=P1(I,J)
C
C 30 CONTINUE
C
C RETURN
C
C END

```

```

C SUBROUTINE UPDSTA(ESTATE,KGAIN,CVPOS)
C (* 434 - UPDATE STATE ESTIMATE *)
C
C CALLS
C MMLT
C CALLED BY
C INCORP
C
C INPUT
C RELPOS,AT,ESTATE
C
C OUTPUT
C ESTATE
C
C REAL CVPOS(3)
C REAL MEASURED CHASE VEHICLE POSITION IN PRIMARY REFERENCE FRAME
C REAL DELTA,KGAIN,POSERR
C REAL ADJUSTMENT TO ESTATE
C REAL ESTATE(6)
C ESTIMATE OF STATE VECTOR
C INTEGER I
C DO LOOP INDEX
C REAL KGAIN(6,3)
C REAL KALMAN GAIN MATRIX
C REAL POSERR(3)
C REAL MEASURED POSITION MINUS PREDICTED POSITION
C
C (* COMPUTE ESTATE=ESTATE+KGAIN*(CVPOS-PREDICTED POSITION) *)
C DO I=1,3
C POSERR(I)=CVPOS(I)-ESTATE(I)
C CALL MMLT(DELTA,KGAIN,POSERR,6,3,1)
C DO I=1,6
C ESTATE(I)=ESTATE(I)+DELTA(I)
C
C 10 CONTINUE
C
C 20 RETURN
C
C END

```

ORIGINAL PAGE IS  
OF POOR QUALITY

```

C SUBROUTINE ESTCOV(ESTATE,R,ACV,ACVT)
C (* 432 - ESTIMATE MEASUREMENT COVARIANCE *)
C CALLS SQR1, DFRD, MMLT
C CALLED BY INCORP
C INPUT ESTATE
C OUTPUT R
C REAL ACV(3,3), ACVT(3,3)
C DIRECTION COSINE MATRIX MEASURED BY IMU, GIVING CHASE VEHICLE
C ATTITUDE, AND THE TRANSPOSE OF THIS MATRIX
C REAL ESTATE(6)
C ESTIMATE OF STATE VECTOR
C DO 10 I=1,3
C INTEGER I,J INDICES
C REAL R(3,3) MEASUREMENT COVARIANCE
C REAL RANGE
C ESTIMATED RANGE TO TARGET SPACECRAFT
C REAL RI(3,3)
C INTERMEDIATE RESULTS
C DO 10 I=1,3
C DO 10 J=1,3
C R(J,I)=0
C RANGE=SQR1(DPR(ESTATE,ESTATE,3))
C RI(1,1)=R E-Z(RANGE-3)**4+.005
C RI(2,2)=R E-Z(RANGE-3)**4+.005
C RI(3,3)=R E-Z(RANGE-3)**4+.005
C CALL MMLT(RI,R1,ACVT,R,3,3,3)
C CALL MMLT(R,R1,ACV,3,3,3)
C RETURN
C END

C SUBROUTINE KALGAN(R,P,G,KGAIN)
C (* 433 - COMPUTE KALMAN GAIN MATRIX *)
C CALLS MADD, MINV, MMLT
C CALLED BY INCORP
C INPUT R,P,G
C OUTPUT KGAIN
C INTEGER I,J
C ERROR CODE (=0 IF NO ERROR)
C PARTIAL OF MEASUREMENT WITH RESPECT TO STATE
C REAL G(3,6)
C REAL GT(3,3)
C TRANSPOSE OF G
C DO 10 I=1,3
C INTEGER I,J INDICES
C REAL KGAIN(6,3)
C KALMAN GAIN MATRIX
C REAL P(6,6)
C STATE ESTIMATE COVARIANCE
C REAL R(3,3) MEASUREMENT COVARIANCE
C REAL SCRATCH(4,6)
C REAL TEMP1(6,3), TEMP2(3,3), TEMP3(3,3)
C INTERMEDIATE RESULTS WITH NO PROBLEM-RELATED SIGNIFICANCE
C INTEGER TERMNL
C FORTRAN UNIT NUMBER FOR TERMINAL
C COMMON/SIMUL/TERMNL, IDUMMY
C DO 10 I=1,3
C DO 10 J=1,6
C GT(I,J)=G(I,J)
C CALL MMLT(TEMP1,P,GT,6,6,3)
C CALL MMLT(TEMP2,G,TEMP1,3,6,3)
C CALL MADD(TEMP3,R,TEMP2,3,3)
C CALL MINV(TEMP2,TEMP3,3,3)
C IF(ERR NE 0) GO TO 20
C CALL MMLT(TEMP1,GT,TEMP2,6,3,3)
C CALL MMLT(KGAIN,P,TEMP1,6,6,3)
C RETURN
C 20 CONTINUE
C (* REPORT ERROR *)
C WRITE(TERMNL,901)
C STOP
C 901 FORMAT('MATRIX INVERSION FAILURE IN SUBROUTINE KALGAN')
C END

```

```

SUBROUTINE UPDCOV(P,KGAIN,G)
(* 455 - UPDATE COVARIANCE MATRIX FROM (P=(I-K*G)*P) *)
CALLS
  MPLY
  INCORP
INPUT
  P,KGAIN,G
OUTPUT
  P
REAL G(3,6)
  PARTIAL OF MEASUREMENT WITH RESPECT TO STATE
INTEGER I,J
  DO LOOP INDICES
REAL K(6,6),GAIN(6,6)
  KALMAN GAIN MATRIX
REAL P(6,6)
  COVARIANCE OF STATE ESTIMATE
REAL TEMP(6,6),PI(6,6)
  INTERMEDIATE RESULTS WITH NO PROBLEM-RELATED SIGNIFICANCE
(* COMPUTE I-KGAIN*)
DO 10 I=1,6
  DO 10 J=1,6
    TEMP(I,J)=P(I,J)-KGAIN(I,J)
10 CONTINUE
DO 20 I=1,6
  CALL MPLY(DELTA,KGAIN,POSERR,6,3,1)
20 CONTINUE
DO 30 I=1,6
  DO 30 J=1,6
    PI(I,J)=P(I,J)
30 RETURN
END
  
```

```

SUBROUTINE UPDSTATE(ESTATE,KGAIN,CVPOS)
(* 454 - UPDATE STATE ESTIMATE *)
CALLS
  MPLY
  INCORP
INPUT
  RELPOS,AT,ESTATE
OUTPUT
  ESTATE
REAL CVPOS(3)
  MEASURED CHASE VEHICLE POSITION IN PRIMARY REFERENCE FRAME
REAL DELTA(6)
  ADJUSTMENT TO ESTATE
REAL ESTATE(6)
  ESTIMATE OF STATE VECTOR
INTEGER LOOP INDEX
REAL KGAIN(6,6)
  KALMAN GAIN MATRIX
REAL POSERR(3)
  MEASURED POSITION MINUS PREDICTED POSITION
(* COMPUTE ESTATE=ESTATE+KGAIN*(CVPOS-PREDICTED POSITION) *)
DO 10 POSERR(I)=CVPOS(I)-ESTATE(I)
10 CONTINUE
CALL MPLY(DELTA,KGAIN,POSERR,6,3,1)
DO 20 I=1,6
  ESTATE(I)=ESTATE(I)+DELTA(I)
20 CONTINUE
RETURN
END
  
```













ORIGINAL PAGE IS  
OF POOR QUALITY

```

C CCCCCCCCCCCCCCCC
SUBROUTINE TABLE2(INDEX2,E)
(*#82,2 FIND COMBINATION OF TABLE ENTRIES THAT SATISFY THRUSTER
SELECTION REQUIREMENTS *)
CALLS
CANOME>
CALLED?
SELECT
INPUT
INDEX?
OUTPUT
E
REAL E(14)
THRUSTER COMMAND ENTRIES FROM THRUSTER SELECT LOGIC
INTEGER INDEX2
THRUSTER TABLE INDEX
-----
* DO SECTION BASED ON INDEX * 100,110,120,130,140,150,160,170,
A 180,190,200,210,220,230,240,250,260),INDEX2
10 E(4)=1 0
E(5)=1 0
GO TO 300
20 E(2)=1 0
E(3)=1 0
GO TO 300
30 E(7)=1 0
E(8)=1 0
GO TO 300
40 E(4)=1 0
E(7)=1 0
E(8)=1 0
GO TO 300
50 E(2)=1 0
E(3)=1 0
E(7)=1 0
GO TO 300
60 E(4)=1 0
E(5)=1 0
GO TO 300
70 E(4)=1 0
E(5)=1 0
E(9)=1 0
GO TO 300
80 E(2)=1 0
E(3)=1 0
E(4)=1 0
E(5)=1 0
GO TO 300
90 E(2)=1 0
E(4)=1 0
GO TO 300
100 E(2)=1 0
E(3)=1 0
E(4)=1 0
E(5)=1 0
GO TO 300
110 E(2)=1 0
E(4)=1 0
E(7)=1 0
E(9)=1 0
GO TO 300
120 E(4)=1 0
E(5)=1 0
E(7)=1 0
E(8)=1 0
GO TO 300
130 E(4)=1 0
E(8)=1 0
GO TO 300
140 E(2)=1 0
E(7)=1 0
GO TO 300
150 E(2)=1 0
E(4)=1 0
E(5)=1 0
E(9)=1 0
GO TO 300
160 E(4)=1 0
E(6)=1 0
GO TO 300
170 E(2)=1 0
E(5)=1 0
GO TO 300
180 E(3)=1 0
E(5)=1 0
GO TO 300
190 E(3)=1 0
E(4)=1 0
E(8)=1 0
GO TO 300
200 E(3)=1 0
E(5)=1 0
E(9)=1 0
GO TO 300
210 E(3)=1 0
E(5)=1 0
E(7)=1 0
E(8)=1 0
E(9)=1 0
GO TO 300
220 E(5)=1 0
E(8)=1 0
GO TO 300
230 E(3)=1 0
E(7)=1 0
GO TO 300
240 E(3)=1 0
E(4)=1 0
E(5)=1 0
E(9)=1 0
GO TO 300
250 E(5)=1 0
E(6)=1 0
GO TO 300
260 E(3)=1 0
E(9)=1 0
GO TO 300
300 RETURN
C END

```





```

C SUBROUTINE FIRTHR(E)
C (* 483 - PUT THRUSTER COMMANDS IN COMMAND PORTS *)
C CALLS <NONE>
C CALLED BY THRUST
C INPUT E
C OUTPUT <NONE>
C REAL E(14)
C THRUSTER COMMAND ENTRIES FROM THRUSTER SELECT LOGIC
C (* TEMPORARY DUMMY SUBROUTINE *)
C RETURN
C END

C SUBROUTINE IMU(STATE,ACV,ACVT,ATRATE)
C (* 490 - SIMULATE IMU MEASUREMENT *)
C CALLS DIRMAT,MADD,MSCL,ANGVEC
C CALLED BY DDCA
C INPUT GO,STATE,FULDIS,INERCV,MEMPTV
C OUTPUT ACV,ACVT,ATRATE
C REAL ACV(3),ACVT(3)
C DIRECTION COSINE MATRIX AND ITS TRANSPOSE FOR MEASURED ATTITUDE
C OF CHASE VEHICLE WITH RESPECT TO PRIMARY REFERENCE FRAME
C REAL ATRATE(3)
C MEASURED ATTITUDE RATES ABOUT CHASE VEHICLE AXES
C REAL FULDIS(3,3)
C TENSOR DESCRIBING FUEL DISTRIBUTION
C REAL INERCV(3,3)
C INERTIA OF CHASE VEHICLE
C REAL INERFL(3,3)
C FUEL INERTIA TENSOR
C REAL INERFA(3,3)
C INERTIA OF CHASE VEHICLE (LOADL)
C REAL MEMPTV
C MASS OF EMPTY CHASE VEHICLE
C REAL INERFA,INERFL,INERCV,ATRATE
C INERTIA, CHASE VEHICLE ATTITUDE QUATERNION IN TRUTH REFERENCE FRAME
C AND CURRENT PRIMARY REFERENCE FRAME, RESPECTIVELY
C REAL STATE(14)
C TRUTH CHASE VEH. E STATE
C REAL TACV(3,3),TAC(3,3)
C CHASE VEHICLE DIRECTION COSINE MATRIX WITH RESPECT TO TRUTH
C COORDINATE SYSTEM AND INVERSE OF THIS MATRIX
C COMMON/REF/GO
C COMMON/MASPRP/FULDIS,INERCV,MEMPTV
C (* SUBTRACT INITIAL ATTITUDE FROM CURRENT ATTITUDE TO GET CURRENT
C ATTITUDE IN PRIMARY REF. FRAME *)
C GP(1)=GO(4)*STATE(10)+GO(3)*STATE(11)-GO(2)*STATE(12)-
C GP(2)=-GO(3)*STATE(10)+GO(4)*STATE(11)+GO(1)*STATE(12)-
C GP(3)=GO(2)*STATE(13)
C GP(4)=GO(2)*STATE(10)-GO(1)*STATE(11)+GO(4)*STATE(12)+
C GP(3)*STATE(13)
C GP(4)=GO(1)*STATE(10)+GO(2)*STATE(11)+GO(3)*STATE(12)+
C GP(4)*STATE(13)
C (* 901 - CONVERT QUATERNIONS TO DIRECTION COSINE MATRICES *)
C CALL DIRMAT(STATE(10),TACV,TACV1)
C CALL DIRMAT(STATE(10),TACV,TACV1)
C (* DETERMINE INERTIA *)
C CALL MSCL(INERFL,FULDIS,3,3,STATE(14)-MEMF1)
C CALL MADD(INERFA,INERCV,INERFL,3,3)
C (* 904 - FIND ANGULAR VELOCITY VECTOR *)
C CALL ANGVEC(INERFA,STATE(7),ATRATE,TACV)
C RETURN
C END

```











ORIGINAL PAGE  
OF POOR QUALITY

```

C SUBROUTINE XFORM(PA,T,TT)
C * 4D1 - TRANSFORM COVARIANCE MATRIX *
CALLS
  CALL MTRN
  CALLED BY
  INCRPA
INPUT
  PA,T,TT
OUTPUT
  PA
INTEGER J,J
DO-LOOP INDICES
REAL PA(7,7)
REAL T(4,4), TT(4,4)
REAL P11(4,4), P12(4,4), P13(4,4), P14(4,4), P21(4,3), P22(4,3),
P23(4,3), P24(4,3), P31(4,3), P32(4,3), P33(4,3), P34(4,3),
P41(4,3), P42(4,3), P43(4,3), P44(4,3)
P11=TT*TT
P12=TT*P11
P13=TT*P12
P14=TT*P13
P21=TT*P21
P22=TT*P21
P23=TT*P22
P24=TT*P23
P31=TT*P31
P32=TT*P31
P33=TT*P32
P34=TT*P33
P41=TT*P41
P42=TT*P41
P43=TT*P42
P44=TT*P43
P11=TT*P11
P12=TT*P12
P13=TT*P13
P14=TT*P14
P21=TT*P21
P22=TT*P22
P23=TT*P23
P24=TT*P24
P31=TT*P31
P32=TT*P32
P33=TT*P33
P34=TT*P34
P41=TT*P41
P42=TT*P42
P43=TT*P43
P44=TT*P44
CALL MTRN(TT,T)
RETURN
END

```

```

C SUBROUTINE XFORM(PA,T,TT)
C * 4D1 - TRANSFORM COVARIANCE MATRIX *
CALLS
  CALL MTRN
  CALLED BY
  INCRPA
INPUT
  PA,T,TT
OUTPUT
  PA
INTEGER J,J
DO-LOOP INDICES
REAL PA(7,7)
REAL T(4,4), TT(4,4)
REAL P11(4,4), P12(4,4), P13(4,4), P14(4,4), P21(4,3), P22(4,3),
P23(4,3), P24(4,3), P31(4,3), P32(4,3), P33(4,3), P34(4,3),
P41(4,3), P42(4,3), P43(4,3), P44(4,3)
P11=TT*TT
P12=TT*P11
P13=TT*P12
P14=TT*P13
P21=TT*P21
P22=TT*P21
P23=TT*P22
P24=TT*P23
P31=TT*P31
P32=TT*P31
P33=TT*P32
P34=TT*P33
P41=TT*P41
P42=TT*P41
P43=TT*P42
P44=TT*P43
P11=TT*P11
P12=TT*P12
P13=TT*P13
P14=TT*P14
P21=TT*P21
P22=TT*P22
P23=TT*P23
P24=TT*P24
P31=TT*P31
P32=TT*P32
P33=TT*P33
P34=TT*P34
P41=TT*P41
P42=TT*P42
P43=TT*P43
P44=TT*P44
CALL MTRN(TT,T)
RETURN
END

```

```

C SUBROUTINE ATMCOV(ESTATE,R)
C (* 403 - ESTIMATE TARGET-ATTITUDE MEASUREMENT COVARIANCE MATRIX *)
C CALLS MIDN,MSCL,SOR1,DPRD
C CALLED BY INCRPA
C INPUT ESTATE
C OUTPUT R
C REAL ESTATE(3)
C ESTIMATED TRANSLATIONAL POSITION OF CHASE VEHICLE IN PRIMARY FRAME
C INTEGER I
C LOOP INDEX
C REAL R(4,4)
C ESTIMATED COVARIANCE OF MEASUREMENT
C REAL ESTIMATED DISTANCE TO TARGET
C REAL V
C ESTIMATED VARIANCE OF ELEMENT OF MEASUREMENT
C RANGE=SOR1(DPRD(ESTATE,3))
C V=1.25E-9*VARIANCE**3+ 0.001
C CALL DCL(R,V)
C R(4,4)=U(01)*V
C RETURN
C END

C SUBROUTINE PRPESTA(PA,ESTA,STEP)
C (* 4E0 - PROPAGATE ATTITUDE ESTIMATE AND COVARIANCE *)
C CALLS MIDN,MSCL,DIRMAT,CMPCD,MADD,MIDN,MTRN,OMLT,FLOAT,SGRT
C CALLED BY DDCA
C INPUT PA,ESTA,STEP
C OUTPUT PA,FGA
C REAL AT(3,3),TRNAT(3,3)
C TARGET ATTITUDE DIRECTION COSINE MATRIX, DERIVED FROM ESTA
C AND ITS TRANSPOSE
C REAL ESTA(7)
C ATTITUDE STATE ESTIMATE
C 1ST 4 ELEMENTS = TARGET ATTITUDE QUATERNION,
C 5TH ELEMENT = TARGET ANGULAR VELOCITY IN PRIMARY FRAME
C ESTIM (1) IS UPDATED (ESTA) BEFORE NORMALIZATION OF QUATERNION
C REAL F(7,7)
C PARTIAL OF D(ESTA)/DT WITH RESPECT TO (ESTA)
C REAL HAV(4)
C HALF TARGET ANGULAR VELOCITY IN CURRENT TARGET FRAME, AUGMENTED
C WITH A ZERO AS FOURTH ELEMENT
C INTEGER LOOP INDICES
C REAL ININV(3,3)
C INVERSE OF TARGET MOMENT-OF-INERTIA MATRIX
C REAL JA(4)
C AUGMENTED COLUMN FROM J(1)*0.5
C REAL ATT(1)
C REAL ATTITUDE ESTIMATE COVARIANCE MATRIX CORRESPONDING TO ESTA(1)
C REAL PH(7,7)
C STATE TRANSITION MATRIX DERIVED FROM F(1)
C REAL G(7,7)
C EMPIRICAL STATE NOISE COVARIANCE MATRIX
C REAL SIPP
C PROPAGATED STATE ESTIMATE OVER WHICH STATE ESTIMATE & COVARIANCE ARE TO BE
C PROPAGATED
C REAL J(3,3),B(4,3),C(4,3),D(3,3,4),V(3),PH(7,7),P(7,7)
C REAL G(4),AL(3),K1(4),M2(4),GTEMP(4)
C INTERMEDIATE RESULTS WITH NO SIMPLE PHYSICAL INTERPRETATION
C COMMON/TGT1/ ININV
C DATA 0.5, E-5, 7*0.5, E-5, 7*0.5, E-5, 7*0.5, E-5, 7*0.5, E-5, 7*
C 4, 7*0.5, 4, 7*0.5, 4,

```

ORIGINAL PAGE IS  
OF POOR QUALITY

















ORIGINAL PAGE IS  
OF POOR QUALITY

```

C SUBROUTINE TRGATT(TRNAT,T)
C (* 905 - COMPUTE TARGET ATTITUDE AS A FUNCTION OF TIME *)
C CALLS SIN, PWLT
C CALLED BY
C FLASH, DOKCHK
C INPUT
C T
C OUTPUT
C TRNAT
C REAL CHGATT(3,3)
C TRANSPOSE OF DIRECTION COSINE MATRIX REPRESENTING TRUE TARGET
C ATTITUDE CHANGE
C INTEGER ITUMBL
C TARGET TUMBLE AXIS--VALUE OF 1, 2, OR 3 REPRESENTS YAW,
C PITCH, OR ROLL TUMBLE
C REAL PHI
C ROTATION ANGLE
C REAL T
C ELAPSED TIME
C REAL TRNAT(3,3)
C TRANSPOSE OF TARGET'S TRUE-ATTITUDE DIRECTION COSINE MATRIX
C REAL TRNATO(3,3)
C REAL TRNAT VALUE OF TRNAT
C REAL TUMBRAT
C TUMBLE RATE (IN RAD/SEC)
C COMMON/ATINFO/TRNATO,ITUMBL,TUMBRAT
C PHITUMBRAT
C (* SELECT APPROPRIATE SET OF FORMULAS FOR TARGET ATTITUDE *)
C GO TO (10,20,30), ITUMBL
C CONTINUE
C (* COMPUTE ATTITUDE CHANGE RESULTING FROM YAW TUMBLE *)
C CHGATT(1,1)=CDS(PHI)
C CHGATT(2,1)=SIN(PHI)
C CHGATT(3,1)=0
C CHGATT(1,2)=0
C CHGATT(2,2)=SIN(PHI)
C CHGATT(3,2)=CDS(PHI)
C CHGATT(1,3)=0
C CHGATT(2,3)=0
C CHGATT(3,3)=1
C GO TO 40
C 10 CONTINUE
C (* COMPUTE ATTITUDE CHANGE RESULTING FROM PITCH TUMBLE *)
C CHGATT(1,1)=CDS(PHI)
C CHGATT(2,1)=0
C CHGATT(3,1)=0
C CHGATT(1,2)=SIN(PHI)
C CHGATT(2,2)=0
C CHGATT(3,2)=0
C CHGATT(1,3)=SIN(PHI)
C CHGATT(2,3)=0
C CHGATT(3,3)=CDS(PHI)
C GO TO 40
C 20 CONTINUE
C (* COMPUTE ATTITUDE CHANGE RESULTING FROM A ROLL TUMBLE *)
C CHGATT(1,1)=1
C CHGATT(2,1)=0
C CHGATT(3,1)=0
C CHGATT(1,2)=0
C CHGATT(2,2)=CDS(PHI)
C CHGATT(3,2)=SIN(PHI)
C CHGATT(1,3)=0
C CHGATT(2,3)=SIN(PHI)
C CHGATT(3,3)=CDS(PHI)
C 30 CONTINUE
C (* COMPUTE TRUE TARGET ATTITUDE *)
C CALL PWLT(TRNAT,TRNATO,CHGATT,3,3)
C RETURN
C END

```

